Virtual Ancestor Reconstruction: revealing the ancestor of modern humans and Neandertals

Aurélien Mounier[1,2*], Marta Mirazón Lahr[1,3]

[1]The Leverhulme Centre for Human Evolutionary Studies, Department of Archaeology and Anthropology, University of Cambridge, Fitzwilliam Street, Cambridge CB2 1QH, United Kingdom.

[2]UMR 7268 ADES, Aix-Marseille Université/EFS/CNRS, Faculté de Médecine - Secteur Nord, CS80011 Bd Pierre Dramard 13344 Marseille, France.

[3]Turkana Basin Institute, Kenya

*Corresponding author: Aurélien Mounier

Tel:

e-mail: am2099@cam.ac.uk

Abstract

The timing and geographic origin of the common ancestor of modern humans and Neandertals remain controversial. A poor Pleistocene hominin fossil record, and the evolutionary complexities introduced by dispersals and regionalisation of lineages have fuelled taxonomic uncertainty, while new ancient genomic data have raised completely new questions. Here, we use maximum likelihood and 3D geometric morphometric methods to predict possible morphologies of the last common ancestor of modern humans and Neandertals from a simplified fully-resolved phylogeny. We describe the fully-rendered 3-dimensional shapes of the predicted ancestors of humans and Neandertals, and assess their similarity to individual fossils or population of fossils of Pleistocene age. Our results support models of an Afro-European ancestral population in the Middle Pleistocene (*H. heidelbergensis sensu lato*) and further predict an African origin for this ancestral population.

Keywords: *H. neanderthalensis*; *H. sapiens*; Last Common Ancestor; *H. heidelbergensis*; 3D geometric morphometrics; maximum likelihood

Fossil discoveries (Arsuaga et al., 1997; Carbonell et al., 2008; Leakey et al., 2012; Villmoare et al., 2015), new analytical methods (Baab, 2008) and, more recently, ancient genomics (Fu et al., 2013; Fu et al., 2014; Meyer et al., 2014; Prüfer et al., 2014; Seguin-Orlando et al., 2014) continuously enhance our understanding of the evolutionary history of the genus *Homo* over the last two million years (Ma). However, no consensus exists regarding major aspects of that history (Wood, 1999; Wood and Lonergan, 2008; Lordkipanidze et al., 2013), partly because of the rarity and fragmentary nature of Pleistocene fossils, partly because of the difficulty in dating material in that time range, and partly because of the emergent complexity revealed by ancient DNA (aDNA) results. Palaeoanthropologists and geneticists must infer evolutionary events from limited samples from different geographical areas and/or time periods, and despite the substantial research effort, even the basic pattern of relationships of a simplified phylogenetic tree remains contentious (Wood and Lonergan, 2008).

Since a strict Multiregional Model of modern human origins (Wolpoff et al., 1994) was abandoned (see, Assimilation Model, Smith et al., 2005), most researchers agree that humans and Neandertals share a last common ancestor (LCA) who lived at some time after early species of *Homo* first dispersed out of Africa. The proposed dates for the LCA range from 1 Ma ago or more to *ca.* 300,000 years ago (ka) (Carbonell et al., 1995; Bermúdez de Castro et al., 1997; Lahr and Foley, 2001; Hublin, 2009; Endicott et al., 2010; Stringer, 2012), and must now accommodate the separation of the elusive Denisovan lineage (Krause et al., 2010; Reich et al., 2010). But the uncertainty goes beyond chronology, with the diversity and number of species and lineages also disputed. Five different species, representing different morphologies and implying different evolutionary processes, have been proposed as including the LCA - *H. erectus, H. antecessor, H. heidelbergensis, H. rhodesiensis,* and *H. helmei* (Carbonell et al., 1995; Bermúdez de Castro et al., 1997; Lahr and Foley, 2001; Hublin, 2009; Mounier et al., 2009; Stringer, 2012; Gómez-Robles et al., 2015). However, the species *H. heidelbergensis*, cladistically a metaspecies (Baum, 1992; Groves and Lahr, 1994), has recently become the focus of most debates on the ancestry of modern humans and Neandertals (Arsuaga et al., 1997; Rightmire, 2008; Mounier et al., 2009; Mounier et al., 2011; Stringer, 2012). *H. heidelbergensis* (Schoetensack, 1908) was proposed in 1908 after the discovery of a morphologically unique jaw in Mauer (Mounier et al., 2009), Germany, now dated to 609±40 ka (Wagner et al., 2010). To some authors, *H. heidelbergensis* (*sensu stricto*) consists of a particular set of Middle Pleistocene (MP) European fossils (Arsuaga et al., 1997; Rosas and Bermúdez de Castro, 1998); to others, the taxon includes the contemporaneous African material (*H. heidelbergensis sensu lato*) (Stringer, 1983; Rightmire, 2008; Mounier et al., 2009; Stringer, 2012), with or without the set of fossils also known as *H. helmei* (Foley and Lahr, 1997).

Evolutionarily, these systematic and chronological differences translate into a range of models. The most extreme argues for a very early separation of European and African lineages from a *H. erectus* ancestor in Africa (or *H. antecessor* in Europe), whereby *H. heidelbergensis* in Europe would evolve into Neandertals through the progressive accretion of apomorphic features (Condemi, 1989; Dean et al., 1998), while *H. rhodesiensis* in Africa would evolve into *H. sapiens* (Arsuaga et al., 1997; Hublin, 2009). This model implies the absence of significant dispersal events between Africa and Europe throughout the Middle Pleistocene, and a large degree of morphological and technological convergence in MP fossils and archaeological industries of both continents; it is also a poor fit to most recent genomic results (Fu et al., 2013). At the other extreme, there is the suggestion that recurrent

dispersals out of Africa would have brought African populations to Eurasia at several points in time, the human-Neandertal LCA representing the last of these before modern humans, namely the recent expansion of a short-lived taxon, *H. helmei*, 250-450 ka (Foley and Lahr, 1997; Lahr and Foley, 1998). Besides implying very different population responses to climate change and biogeographical dynamics, this model also requires a degree of morphological convergence, in this case between early and late MP fossils of Europe. Nevertheless, it accounts for the shared technological trajectories across Africa and Europe, and approximates recent aDNA results that suggest humans and Neandertals share a mitochondrial DNA (mtDNA) ancestor more recently than Denisovans and MP European fossils, such as Sima de los Huesos in Atapuerca (Fu et al., 2013; Meyer et al., 2014). In between these two models, there are various formulations that work on the premise that before the dispersal of modern humans in the recent past, there was only one major other dispersal event from Africa to Eurasia early in the Middle Pleistocene (~700 ka), establishing populations of *H. heidelbergensis* in each continent, which then evolved into Neandertals in Europe and modern humans in Africa, as well as presumably, Denisovans in Asia (Rightmire, 2008; Mounier et al., 2009; Mounier et al., 2011; Stringer, 2012). This model accounts for patterns of morphological continuity in the European fossil record, although it implies important technological convergences, and a mis-match with mtDNA and genomic data (Fu et al., 2013; Meyer et al., 2014).

These models are not only different from one another, but they are also very general; ancient genomic data have highlighted that population processes may be more complicated than implied by any of these models and that greater precision is required to understand the turnover between Neandertals and modern humans (Meyer et al., 2014). However, this complex picture of the phylogenetic histories of Neandertals and modern humans can be summarized through three simplified models (Fig. 1):

1. A late Lower Pleistocene common ancestry - this model supports deep regional chrono-species within a morphological accretion model – *H. antecessor-heidelbergensis-neanderthalensis* in Europe*, H. rhodesiensis*-(*helmei*)-*sapiens* in Africa. In this framework, the LCA may be distant from both terminal taxa and resemble early *Homo* (Carbonell et al., 1995; Bermúdez de Castro et al., 2004; Carbonell et al., 2005; Carbonell et al., 2008).

2. An early Middle Pleistocene common ancestry - model 2 supports the presence of shared derived features between European *H. heidelbergensis* and Neandertals, especially in the face. The model is consistent with the older extreme of the age-range estimate of the Neandertal-*sapiens* split based on genomic data (Prüfer et al., 2014), but is incompatible with ancient mtDNA evidence pointing to a (Neandertal-*sapiens*)/(European (?) *H. heidelbergensis*-Denisovan) structure. In this framework, the LCA may be equally distant from both terminal taxa and resemble MP specimens, supporting *H. heidelbergensis sensu lato* as the ancestral species (Rightmire, 2008; Mounier et al., 2009; Stringer, 2012).

3. A mid-Middle Pleistocene common ancestry - model 3 is compatible with the younger age extreme of the age-range estimated for the split Neandertal-*sapiens* based on genomic data, and shared derived technological innovations in humans and Neandertals, but it is inconsistent with ancient mtDNA evidence and with the observed regional morphological patterns of similarities in the face of European *H. heidelbergensis* and Neandertals. In this hypothesis, the

LCA should be closer to African MP fossils than to European MP ones who are removed from the Neandertal lineage (Lahr and Foley, 1998).

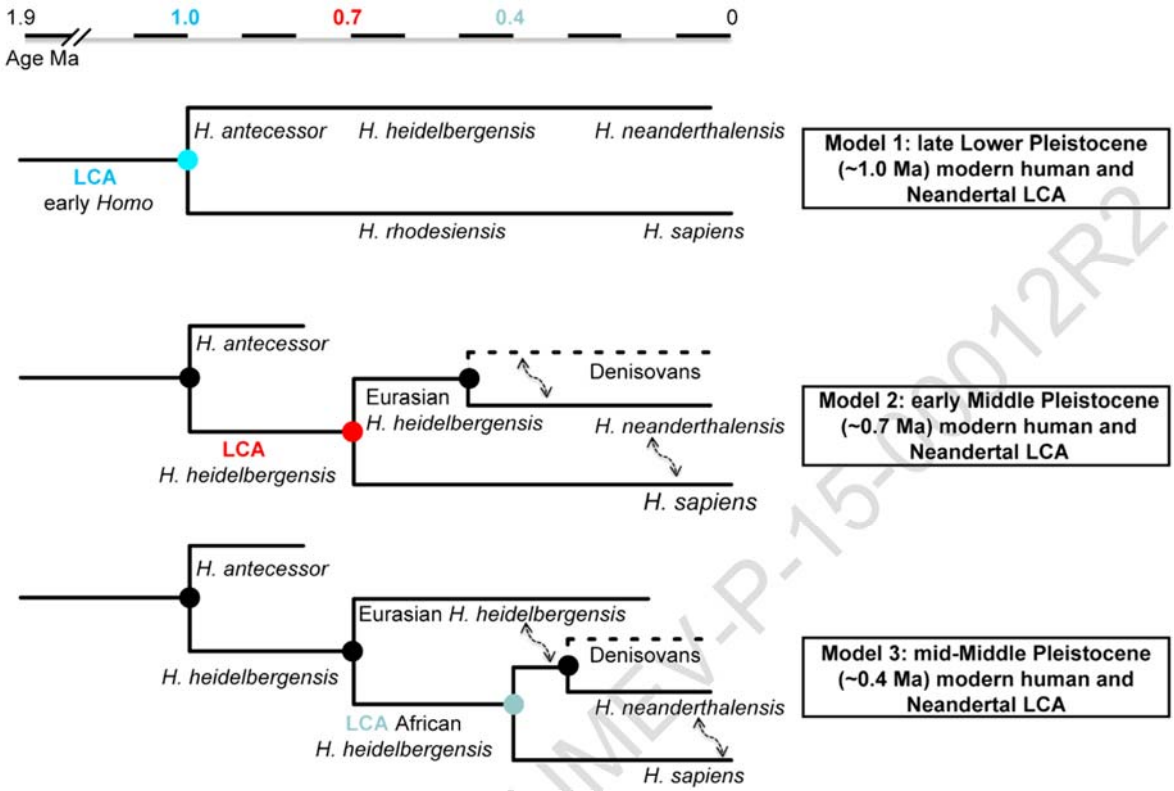

Figure1. Three possible phylogenetic histories of Neandertals and modern humans. Model 1: consistent with the concept of regional chrono-species within a morphological accretion model – *H. antecessor-heidelbergensis-neanderthalensis* in Europe, *H. rhodesiensis*-(*helmei*)-*sapiens* in Africa. Model 2: consistent with shared derived features of European *H. heidelbergensis* and Neandertals, especially in the face and with the older extreme of the age-range estimate of the split Neandertal-*sapiens* based on genomic data; incompatible with ancient mtDNA results pointing to a (Neandertal-*sapiens*)/(European (?) *H. heidelbergensis*-Denisovan) structure, and shared derived technological innovations in modern humans and Neandertals. Model 3: compatible with younger extreme of the age-range estimated for the split Neandertal-*sapiens* based on genomic data, and shared derived technological innovations in humans and Neandertals, but inconsistent with ancient mtDNA evidence and with regional morphological patterns of similarities in the face of European *H. heidelbergensis* and Neandertals. The blue, red and grey circles represent the possible LCAs to AMHs and Neandertals, the black circles represent other LCAs of the phylogenetic hypotheses.

One of the stumbling blocks to resolving these different interpretations is the paucity of MP fossil remains, particularly in Africa. Here, we predict the morphology of hypothetical ancestors on the basis of phylogenetic hypotheses. These virtual fossils are fully-rendered 3D models that can be, in turn, analysed and compared to the actual fossil record. Approaches to predict ancestral states of continuous characters are well-known in biological sciences and have been applied before (Madison, 1991; Martins and Hansen, 1997; Rohlf, 2001; Wiley et al., 2005; Polly, 2008), but only rarely to human evolution itself. An exception is the study of Gómez-Robles et al. (2013) who applied a generalized linear model (GLM) within a Brownian motion model of evolution (Edwards and Cavalli-Sforza, 1964;

Felsenstein, 1985, 1988; Madison, 1991; Pagel, 2002) to predict ancestral morphologies of hominin teeth in a two dimensional morphospace.

In the present study, we apply a similar method to the divergence between the modern human and Neandertal lineages (Beerli and Edwards, 2002; Endicott et al., 2010). We use maximum likelihood (Felsenstein, 1981; Schluter et al., 1997) and 3D geometric morphometric techniques to generate fully-rendered 3D models representing the shape of virtual last common ancestors (vLCAs) from a fully-resolved phylogenetic hypothesis depicting the relationships of hominin species within the genus *Homo.* This simplified phylogeny uses African early *Homo* fossils as outgroup of two sister taxa: modern humans and Neandertals which share a common ancestor in the Pleistocene (see, Methods, Fig. 2 and Table 1). The Neanderthal and modern human lineages that extend back through the Pleistocene to their last common ancestor have a complex and to some extent unknown combination of both evolutionary change (Lahr and Foley, 1998; Reyes-Centeno et al., 2014) and population substructure (Fabre et al., 2009). To avoid ambiguities of these unknown parameters our reconstruction is not based directly on MP fossils.

To test these competing hypotheses, we constructed a vLCA of modern humans and Neanderthals using parameters derived from each of these three models (Fig. 1 and 2). The morphologies of these vLCAs are then compared to a larger dataset of early *Homo*, MP fossils, Neandertals and AMHs through geometric morphometric analyses on the calvarium and the upper face (see, Methods).

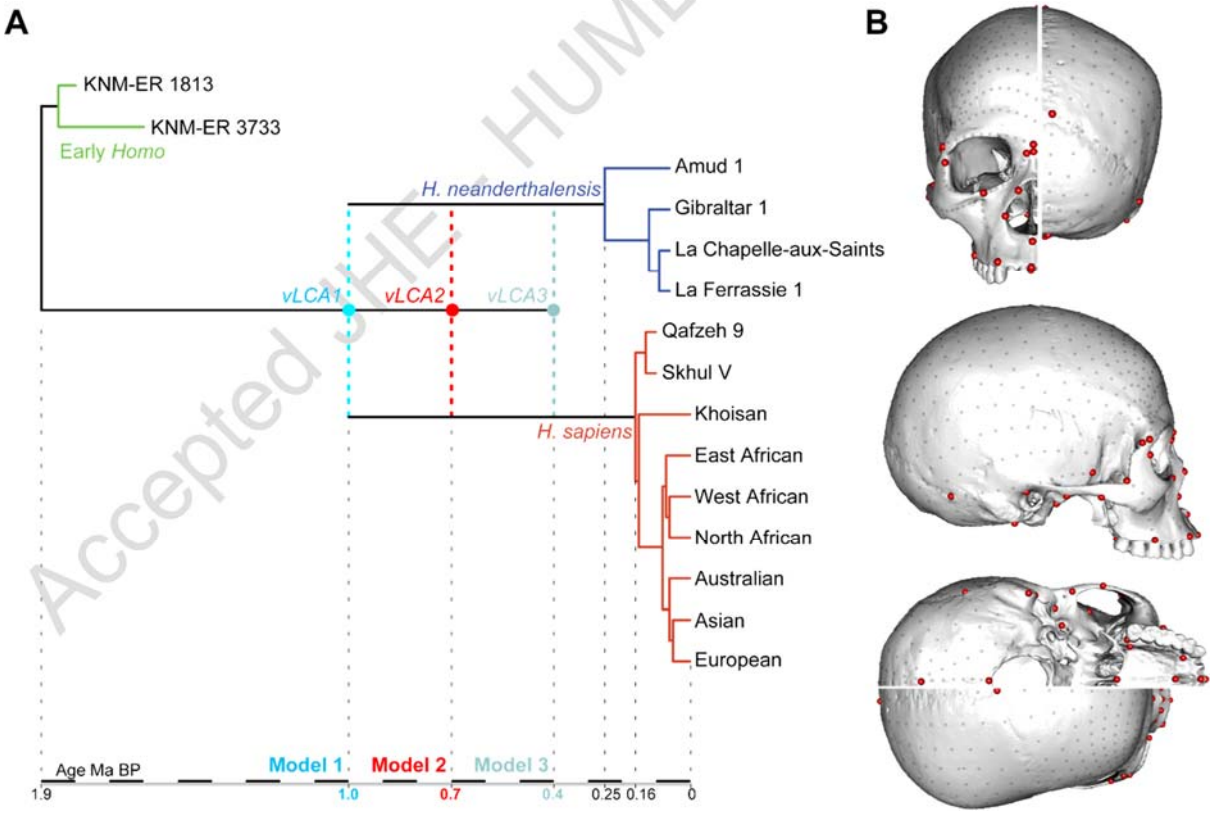

Figure 2. (A) Cladogram depicting the fully-resolved phylogeny of the genus *Homo.* In green two African early *Homo* specimens, used as an outgroup to the two sister clades: *H. neanderthalensis* in blue and *H. sapiens* in red. The vLCA of these two sister taxa has been computed for three distinct chronologies (Fig. 1): 1) late Lower

Pleistocene (model 1); early Middle Pleistocene (model 2); and mid-Middle Pleistocene (model 3). (B) Khoisan half-cranium depicting the landmarks (red) and semi-landmarks (grey) used to perform the General Procrustes Analysis (GPA) and the Principal Component Analysis (PCA) from which the ancestral shapes are computed.

Materials and Methods

Materials

The analysis needs two different samples: a sample of 3D models to build the hypothetical phylogeny and to calculate the morphology of the vLCAs of the cladogram, and a comparative sample to test and compare the morphology of the vLCAs to the actual fossil record.

The specimens used to calculate the vLCAs (Table 1) are two fossils of early *Homo*, four Neandertals and nine modern humans, including the Skhūl V and Qafzeh 9 specimens. The 3D models were built following two procedures: 1) medical computed tomographic scans (voxel size between 0.449219 and 0.488281 mm) for the nine modern humans (Duckworth Collection, University of Cambridge), Skhūl V (Peabody Museum of Archaeology and Ethnology, Harvard University), La Ferrassie 1 and La Chapelle-aux-Saints (Musée de l'Homme, Paris), which were processed in Amira (v5.5, FEI); 2) surface scanned specimens (the remaining sample) using an optical scanner (HDI Advance, 45µ accuracy, LMI) and the FlexScan 3D software (v.3.3, LMI). The resulting models (on average 1.5 million vertices) are described by 797 landmarks, collected using the Landmark software (IDAV, Wiley, 2005), among which 744 are semi-landmarks (116 on curves located on the face and 628 on surfaces located on the calvarium) which are allowed to slide (see, Figure 2B and Gunz et al., 2005; Gunz and Mitteroecker, 2013). The configuration of landmarks describes the whole cranium: 43 are positioned on the midline and 377 on each side and base. We created two sets of landmarks, left and right, of 420 landmarks (32 landmarks, 58 curve semi-landmarks on the face and 330 surface semi-landmarks on the calvarium, Fig. 2B). Missing landmarks were estimated by mirroring existing landmarks on the other side. In order to correct for bilateral asymmetry in each specimen, the right and left configurations were aligned using a Generalized Procruste analysis (GPA, Gower, 1975; Rohlf and Slice, 1990) and the mean coordinates of the 420 landmarks were used to perform subsequent analyses.

Table 1. Specimens used to compute the vLCA.

Specimens	Chronology		Site	3d models	Institution
Early Pleistocene					
KNM-ER 1813	1.86±0.08 Ma	(Feibel et al., 2009)	Koobi Fora, East Turkana, Kenya	HDI	NKM
KNM-ER 3733	~1.6 Ma	(Gathogo and Brown, 2006)	Koobi Fora, East Turkana, Kenya.	HDI	NKM
Late Pleistocene					
Homo neanderthalensis					
Gibraltar 1	45-70 ka	(Oakley, 1964)	Forbes' Quarry, Gibraltar	HDI	DC
La Ferrassie1	53-66 ka	(Blackwell et al., 2007)	La Ferrassie, France	CT	MH
La Chapelle-aux-Saints	~50 ka	(Boule, 1911-1913)	La Chapelle-aux-Saints, France	CT	MH
Amud 1	50-60 ka	(Bar-Yosef, 1998)	Amud, Israel	HDI	DC
Homo sapiens					
Qafzeh 9	100-130 ka	(Grün and Stringer, 1991)	Qafzeh, Israel	HDI	DC
Skhūl V	88-117 ka	(Grün et al., 2005)	Skhūl, Israel	CT	PM
Holocene					
Khoisan (AF 1144)	XIX century	-	South-Africa (Duckworth, Cambridge)	CT	DC
East-African (AF 15.032)	XIX century	-	Somalia (Duckworth, Cambridge)	CT	DC
West-African (AF 1088)	XIX century	-	Congo (Duckworth, Cambridge)	CT	DC
Nubian (NU 761)	~4000 BP	-	Sudan (Duckworth, Cambridge)	CT	DC
Australian (Aus 108)	XIX century	-	Australia (Duckworth, Cambridge)	CT	DC
Asian (AS 21.0.7)	XIX century	-	China (Duckworth, Cambridge)	CT	DC
European (Eu 42.00.2)	XIX century	-	Italy (Duckworth, Cambridge)	CT	DC

The '3d models' column indicates whether the 3d models were obtained using CT scans or were scanned using an optical scanner (HDI advance); the 'Institution' column indicates where the specimens are kept and where they were scanned (NKM: National Kenyan Museums, Nairobi; DC: Duckworth Collection, Cambridge; MH: Musée de l'Homme, Paris; PM: Peabody Museum, Cambridge). Bold types indicate that original specimens were examined.

The comparative sample is composed of 46 fossils from Africa, Asia and Europe and was selected to encompass as much of the Pleistocene hominin record as possible (Table 2). It includes nine early *Homo* specimens, 12 *H. neanderthalensis*, seven *H. sapiens* and 16 MP specimens. With the exception of those fossils listed in Table 1 - two early *Homo* (KNM-ER 1813 and 3733), four Neandertals (La Ferrassie 1, La Chapelle-aux-Saints, Gibraltar 1 and Amud 1) and the Skhūl V and Qafzeh 9 fossils, the remaining specimens were not used to compute the shape of the vLCAs; in particular, none of the MP specimens were used in the hypothetical phylogenetic tree (Fig. 2, Table 1). No juveniles were included with the exception of D2700 and KNM-WT 15000 due to the scarcity of complete fossils available in the Early Pleistocene. To increase the modern human comparative sample, 18 Holocene *H. sapiens* crania were also included (eight Neolithic and 10 historic individuals). The data of the comparative sample include 14 landmarks on the calvarium (Table C.1, Fig. 4) and 8 landmarks on the upper face (Table C.2, Fig. 5).

Table 2. Specimens used in the comparative geometric morphometric analysis.

Specimens	Chronology		Site	Analyses PCA	Labels Fig. 4-7
Early Pleistocene					
D2280	1.81±0.05 Ma	(de Lumley et al., 2002)	Dmanisi, Georgia	Cal	-
D2700	1.81±0.05 Ma	(de Lumley et al., 2002)	Dmanisi, Georgia	Cal,Uf	-
KNM-ER 1813	1.86±0.08 Ma	(Feibel et al., 2009)	Koobi Fora, East Turkana, Kenya	Cal,Uf	ER1813
KNM-ER 1470	~1.8 Ma	(Tamrat et al., 1995)	Koobi Fora, East Turkana, Kenya	Cal,Uf	ER1470
OH 24	~1.8 Ma	(Gathogo and Brown, 2006)	Olduvai Gorge, Tanzania	Uf	-
KNM-ER 3733	~1.6 Ma	(Gathogo and Brown, 2006)	Koobi Fora, East Turkana, Kenya.	Cal,Uf	ER3733
KNM-ER 3883	~1.6 Ma	(Brown and McDougall, 1993)	Koobi Fora, East Turkana, Kenya	Cal	ER3883
KNM-WT 15000	~1.6 Ma	(Larick et al., 2001)	Nariokotome, West Turkana, Kenya	Cal,Uf	WT15000
Sangiran 17	1-1.5 Ma	(de Lumley et al., 2002)	Sangiran, Java, Indonesia	Cal,Uf	S17
Middle Pleistocene					
SH5	427±12 ka	(Arnold et al., 2014)	Sima de los Huesos, Atapuerca, Spain	Cal,Uf	-
Arago 21	450 ka	(Yokoyama, 1989)	Tautavel, France	Uf	-
Ceprano	385-430 ka	(Manzi et al., 2010)	Ceprano, Italy	Cal	-
Petralona	150-250 ka	(Grün, 1996)	Petralona, Greece	Cal,Uf	-
Steinheim	250 ka	(Adam, 1985)	Steinheim, Germany	Cal,Uf	-
Ehringsdorf H	230 ka	(Blackwell and Schwarcz, 1986)	Ehringsdorf, Germany	Cal	-
Dali	260-300 ka	(Yin et al., 2001)	Dali, China	Cal,Uf	-
Jinniu Shan	200 ka	(Chen, et el. 1994)	Jinniu Shan, China	Cal,Uf	-
Bodo	600 ka	(Clark et al., 1994)	Bodo, Ethiopia	Uf	-
Ndutu	200-400 ka	(Leakey and Hay, 1982)	Ndutu, Tanzania	Uf	-
KNM-ES 11693	200-300 ka	(Bräuer and Leakey, 1986)	Eilye Springs, Kenya	Cal	ES11693
Kabwe	> 125 ka	(Stringer, 2011)	Kabwe, Zambia	Cal,Uf	-
Jebel Irhoud 1	190-130ka	(Grün and Stringer, 1991)	Jebel Irhoud, Algeria	Cal,Uf	Irhoud1
Florisbad	259±35 ka	(Grün et al., 1996)	Bloemfontein, South Africa	Uf	-
LH 18	129-108 ka	(Manega, 1995)	Laetoli, Tanzania	Cal	-
Omo II	~130 ka	(McDougall et al., 2008)	Omo Kibish, Ethiopia	Cal	-
Singa	133±2 ka	(McDermott et al., 1996)	Singa, Sundan	Cal	
Late Pleistocene					
Homo neanderthalensis					
Saccopatore 1	130-120 ka	(Bruner and Manzi, 2006)	Saccopastore, Italy	Cal	Sacc1
Saccopastore 2	130-120 ka	(Bruner and Manzi, 2006)	Saccopastore, Italy	Uf	Sacc2
Gibraltar 1	45-70 ka	(Oakley, 1964)	Forbes' Quarry, Gibraltar	Cal,Uf	G1
La Ferrassie1	53-66 ka	(Blackwell et al., 2007)	La Ferrassie, France	Cal,Uf	LF1
La Quina H5	~65 ka	(Mellars, 1996)	La Quina, France	Cal	LQH5
Guattari I	52±12 ka	(Grün and Stringer, 1991)	Monte Circeo, Italy	Cal,Uf	Gual
La Chapelle-aux-Saints	~50 ka	(Boule, 1911-1913)	La Chapelle-aux-Saints, France	Cal,Uf	LCS
Spy 1	>36 ka	(Toussaint and Pirson, 2006)	Spy, Belgium	Cal	-
Saint Césaire	36 ka	(Mercier et al., 1991)	Saint Césaire, France	Uf	StC
Tabūn C1	122±16 ka	(Grün and Stringer, 2000)	Tabūn, Israel	Cal,Uf	TC1
Shanidar V	60-80 ka	(Trinkaus, 1991)	Shanidar, Irak	Uf	ShV
Amud 1	50-60 ka	(Bar-Yosef, 1998)	Amud, Israel	Cal,Uf	A1
Homo sapiens					
Cro-Magnon I	28 ka	(Henry-Gambier, 2002)	Les Eyzies, France	Uf	CMI
Abri Pataud	22 ka	(Bricker and Mellars, 1987)	Les Eyzies, France	Cal,Uf	AP
Chancelade	~12 ka	(Grün and Stringer, 1991)	Chancelade, France	Cal,Uf	Ch
Qafzeh 9	100-130 ka	(Grün and Stringer, 1991)	Qafzeh, Israel	Cal,Uf	Q9
Qafzeh 6	90-130 ka	(Grün et al., 2005)	Qafzeh, Israel	Cal,Uf	Q6
Skhūl V	66-102 ka	(Grün et al., 2005)	Skhūl, Israel	Cal	SV
Ohalo II	19 ka	(Carmi and Segal, 1992)	Ohalo, Israel	Cal,Uf	OII
Holocene					
Neolithic					
Saharan 1 (MN10H3)	6970 ± 130 BP	(Dutour, 1989)	Hassi-el-Abiod, Mali	Cal,Uf	1
Saharan 2 (MN10H1)	6970 ± 130 BP	(Dutour, 1989)	Hassi-el-Abiod, Mali	Cal,Uf	2
Saharan 3 (MN6H1)	6970 ± 130 BP	(Dutour, 1989)	Hassi-el-Abiod, Mali	Uf	3
Saharan 4 (MN36BH13)	6970 ± 130 BP	(Dutour, 1989)	Hassi-el-Abiod, Mali	Cal	4
French 1 (B2 n°33)	3740 ± 120 BP	(Dutour, 1994)	Loisy-en-Brie, France	Cal,Uf	5
French 2 (D3 n°3)	3740 ± 120 BP	(Dutour, 1994)	Loisy-en-Brie, France	Cal	6
French 3 (C2 n°28)	3740 ± 120 BP	(Dutour, 1994)	Loisy-en-Brie, France	Uf	7
French 4 (D3 n°2)	3740 ± 120 BP	(Dutour, 1994)	Loisy-en-Brie, France	Uf	8
Historic					
English 1 (2708)	XVIII-XIX centuries	(Molleson and Cox, 1993)	Spitalfields, United Kingdom	Cal,Uf	9
English 2 (2728)	XVIII-XIX centuries	(Molleson and Cox, 1993)	Spitalfields, United Kingdom	Cal	10
Romanian 1 (17443)	XIX century	-	Romania (MNHN, Paris)	Cal,Uf	11
Romanian 2 (17459)	XIX century	-	Romania (MNHN, Paris)	Cal	12
Chinese 1 (7.6991)	XX century	-	China (NHM, London)	Cal,Uf	13
Chinese 2 (7.6993)	XX century	-	China (NHM, London)	Cal,Uf	14
Indonesian 1 (8.3785)	XX century	-	Java (NHM, London)	Cal,Uf	15
Indonesian 2 (8.34)	XX century	-	Java (NHM, London)	Cal,Uf	16

Nigerian 1 (AF 23.294)	XX century	-	Nigeria (NHM, London)	Cal,Uf	17
Nigerian 2 (AF 23.293)	XX century	-	Nigeria (NHM, London)	Cal,Uf	18

Column "Analyses" indicates in which geometric morphometric analyses the specimens were included: analysis of the calvarium (Cal) or of the upper face (Uf). Bold types indicate that original specimens were examined.

Methods

Reconstructing the hypothetical LCAs. To compute the ancestral form of the continuous shape variables, we use an explicit model of evolutionary change assuming random walks in continuous time: the Brownian motion model of evolution (Edwards and Cavalli-Sforza, 1964; Felsenstein, 1985, 1988; Madison, 1991; Pagel, 2002). Following Schluter and colleagues (1997: 1700) a model assuming random walks in continuous time presents three main features: "*(1) the probability of change at a point in time along any branch of the phylogeny depends only on the character state at that time, and not on prior character states; (2) transitions along each branch are independent of changes elsewhere in the tree; and (3) rates of change are constant throughout time and along all branches. We estimate these rates from the tree and current species values, rather than from prior knowledge or belief*". Within this framework we use the maximum likelihood approach (Felsenstein, 1981; Schluter et al., 1997) to compute ancestral states.

To generate the ancestral shapes, we use a fully-resolved simplified phylogeny of the genus *Homo* (Fig. 2A): two early *Homo* specimens (KNM-ER 1813, KNM-ER 3733) compose the outgroup of the two sister taxa, the Neandertals (((La Ferrassie 1, La Chapelle-aux-Saints) Gibraltar 1) Amud1) and the modern humans ((Qafzeh 9, Skhūl V) (Khoisan, (East African (West African, Nubian)) (Australian (Asian, European)))). The structure of the Neandertal clade reflects potential sub-groups in the population (Fabre et al., 2009): 'classic' Western Neandertals (La Ferrassie 1, La Chapelle-aux-Saints), more derived than southern (Gibraltar 1) and Near-Eastern (Amud 1) individuals. The modern human clade is a simplification of our evolutionary history (Lahr and Foley, 1998; Reyes-Centeno et al., 2014): Qafzeh 9/Skhūl V as a sister group to recent *H. sapiens* (Vandermeersch, 1981), which are arranged following their relative genetic relationships - the Khoisan individual outside a clade containing two branches: other Africans (East African (West African, Nubian)) and Eurasians (Australian (Asian, European)). The terminal taxa are positioned in relation to their chronology. The nodes of the phylogeny reflect consensual chronologies based on genetic and palaeoanthropological data. We use three chronological models for the position of the LCA of modern humans and Neandertals, thus computing three distinct hypothetical shapes of the vLCA (see, Fig. 1 and 2, Endicott et al., 2010). The ancestral trait reconstruction was based on all the continuous variables from each terminal taxon separately, and necessitated uncorrelated variables. Accordingly, we used principal components drawn from the original landmark dataset as the continuous variables for the vLCA reconstruction (i.e. 14 PCs, see Table A.1). These PCs represent the shape variables for each specimen obtained after performing a GPA (Gower, 1975; Rohlf and Slice, 1990) and a PCA on the 420 landmark sets of the terminal taxa. The ancestral shape was reconstructed individually for each of the uncorrelated and continuously distributed principal components. We did not use the eigensurface analysis (Polly, 2008; Polly and MacLeod, 2008) as the 3D models' mesh were obtained through two different procedures (see, above).

The approach used in the current study differs from the *Evolutionary Morphing* method presented in 2005 by Wiley and colleagues (Wiley et al., 2005). First, we do not compute directly the 'ancestral' coordinates of the landmarks, but instead use the PCs; second, we use a maximum likelihood method

as an alternative to the methods based on the principle of parsimony. Maximum likelihood reconstructs the ancestral states to maximize the probability of the states observed among the known taxa (in this case, the original Neandertal and *H. sapiens* samples used), following a statistical evolutionary divergence model (Pagel, 1999), in our case a Brownian motion model (Schluter et al., 1997). The maximum likelihood approach computes for each node of the phylogeny the most likely hypothetical ancestral shape variables along with a 95% confidence ellipsoid representing other possible shapes (Fig. 3). The confidence ellipsoid is a quantification of the uncertainty based on a standard probabilistic measure that depends on the rate of variance of the characters, the length of the branches and the topology of the phylogeny. In the case of a deep ancestry between two sister taxa, the uncertainty is larger and the possible ancestral shapes more numerous; a more recent common ancestry will present less uncertainty (Schluter et al., 1997; Polly, 2001). The obtained ancestral scores of each node are rotated back to the original landmark space (Rohlf, 2001; Polly, 2008) in order to obtain new sets of 3D coordinates representing the shape of each node as well as extremes of the 95% confidence ellipsoids.

In order to compare the hypothetical ancestral shapes to the fossil record a further step is necessary. Most Middle Pleistocene fossils are highly fragmented, and very few are sufficiently well preserved to allow a direct comparison based on the 420 landmarks used to compute the ancestors. Thus, we computed the surface of the hypothetical ancestors by warping the surface of one of the terminal taxa (in this case the Khoisan 3D model) onto the shapes described by the generated landmark sets corresponding to the hypothetical ancestors using a thin-plate spline interpolation (Bookstein, 1989, 1991, 1997; Gunz, 2005) (Fig. 3). From these virtual ancestors (vLCAs) we can collect additional landmarks (Landmark software, IDAV, Wiley, 2005) in order to compare them to the actual fossil record.

Geometric morphometric analyses. The Pleistocene fossil record is fragmentary. Therefore, in order to compare the vLCAs to the largest fossil sample possible, we divided our comparative sample in two sub-samples: one focusing on the calvarium described by 14 landmarks (Fig. 4, Table C.1) and one focusing on the upper face described by 8 landmarks (Fig. 5, Table C.2). The landmarks were selected to characterise the calvarium and upper face morphology as well as possible, while taking into consideration the state of preservation of the fossils (Mounier, 2009; Mounier et al., 2011; Mounier, 2012). For each sub-sample, we ran a GPA (Gower, 1975; Rohlf and Slice, 1990) and a Principal Component Analysis based on the procrustes residuals in order to explore the shape affinity of the vLCAs (Fig. 4 and 5).

In order to better assess the affinity of the vLCAs to the fossil record, we calculated the minimum spanning trees (MSTs) of our samples, based on the procrustes distances between the specimens. MSTs methods highlight the relationships in a population by linking together the most closely related specimens, and are commonly used in evolutionary studies (Excoffier and Smouse, 1994; Teixeira et al., 2015). Additionally, we compared the procrustes distances of the vLCAs to each Middle Pleistocene specimen and to each group of fossils, i.e. Early *Homo*, *H. neanderthalensis*, *H. sapiens* and Middle Pleistocene sample, which was further divided into two geographic groups: Eurasians and Africans (Tables 3).

All the analyses were performed on the R platform using the Morpho (version 2.1; Schlager, 2013) and geomorph (version 2.1.2; Adams and Otárola-Castillo, 2013) packages for the 3D geometric morphometric analyses, the ape package (version 3.2; Paradis et al. 2004) for the ancestral state reconstruction, and the phytools package (version 0.4-3.1; Revell, 2012) for visualisation of the phylogenies in morphospace.

Results

Virtual ancestor of *H. sapiens* and *H. neanderthalensis*. The results of the computed virtual ancestors of *H. sapiens* and *H. neanderthalensis* are displayed in Figure 3. We obtained three distinct shapes corresponding to the chronological models (model 1: vLCA1 in blue; model 2: vLCA2 in red, and model 3: vLCA3 in grey).

The three specimens are broadly similar in their morphology and the main trends can be described as follows (Fig. 3D and Appendix B): in *norma lateralis* the vault is low and elongated, the zygomatic is slightly curved backward with a *tuberculum marginale*, the external auditory meatus shows an intermediate position in relation to the zygomatic process and the mastoids are weakly-developed; the frontal shows a well-developed supraorbital region with associated well-developed sinuses; the occipital has a slight occipital bun, it is rounded in *norma occipitalis,* presents an incipient supra-iniac fossa and the maximum width of the calvarium is at the supramastoid crest; the upper face is long and projecting, the maxilla is not pneumatised as observed in Neandertals (Maureille, 1994), but its anterior surface shows the presence of a slight *incurvatio horizontalis*, *sagittalis*, and in *norma facialis* a weakly-marked *incurvatio inframalaris frontalis* is observed. The morphology of the 3 vLCAs' calvaria has been described in some MP specimens such as Kabwe and Petralona (Mounier, 2009), while aspects of the face (such as the *incurvatio inframalaris frontalis*) are reminiscent of the morphology of African and European MP fossils such as Kabwe, Bodo, Arago 21 and Petralona (Mounier, 2009, 2011).

vLCA1 differs from the other ancestors in having a more projecting lower face, a better-developed lateral supraorbital region associated with a less-developed glabella, a larger maximum cranial breadth at the supramastoid crest level, and a longer, less flexed basicranium. vLCA2 and vLCA3 tend to show a larger and more rounded braincase and a more projecting mid-face, especially in vLCA3, as seen in Neandertals (Maureille, 1994).

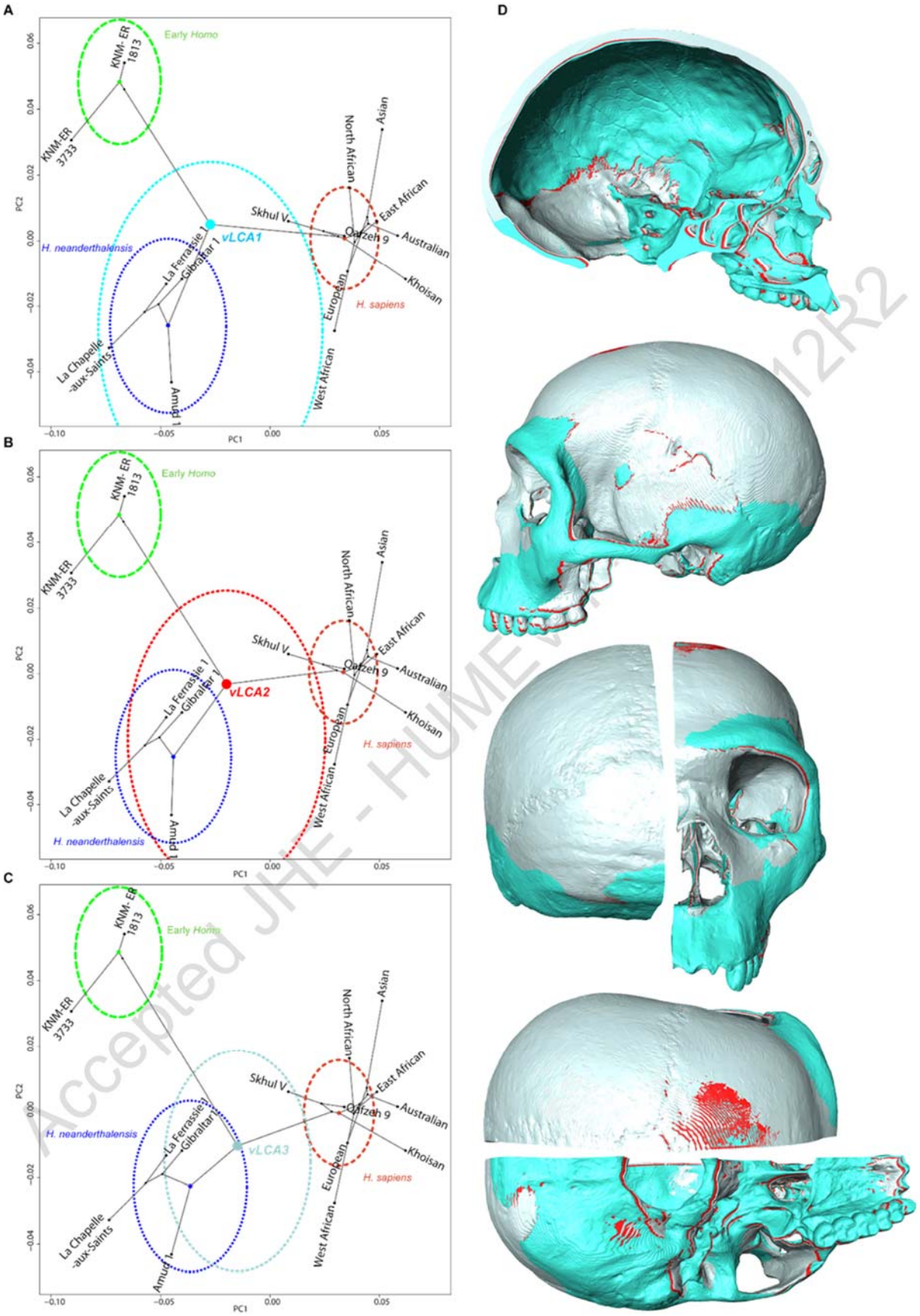

Figure 3. (A, B and C) Projection in morphospace of the three phylogenetic trees corresponding to the three chronological models for the vLCA. Ellipsoids correspond to the 95% confidence interval for each node (i.e. ancestor) of the phylogenies. Model 1 (A, blue) shows a vLCA closer to the early *Homo* clade with an extreme

95% confidence ellipsoid which includes the total variation of the Neandertal clade; model 2 (B, red) shows a vLCA closer to the Neandertal and modern human clades, with a less extreme 95% confidence ellipsoid, which still includes most of the Neandertal morphological variation as well as a part of the modern human variation; model 3 (C, grey) shows a vLCA much closer to Neandertals and modern humans with a 95% confidence ellipsoid which includes *ca.* half of the Neandertal morphological variation, while excluding the modern human morphologies to the exception of the Skhūl V specimen. D depicts the actual morphology of the three aligned vLCAs. vLCA1 (blue) presents a more projecting lower face, lateral brow ridges and lower temporal as well as smaller braincase; vLCA2 (red) presents an intermediate morphology; vLCA3 (grey) presents a less projecting lower face, lateral brow ridges, a more rounded and developed braincase and a more projecting mid-face.

Morphological affinity of the vLCA. Figure 4 shows the two first PCs (54.64% of the total variance) of the PCA based on the procrustes residuals of the analysis of the calvarium (Tables C.1 and C.3). On PC1, the early *Homo* specimens present a low braincase with strong supraorbital torus, a marked postorbital constriction and a low positioned maximal cranial breadth, isolating them from both Neandertals and modern humans. On PC2, the Neandertals show a low and elongated braincase, with a medially placed maximum cranial breadth separating them from the rest of the sample. Among the MP specimens, the more recent fossils approximate modern humans (i.e. Singa, LH18 and Jebel Irhoud 1) and Neandertals (i.e. Steinheim and Ehringsdorf H) in morphospace, while the others tend to be more similar to early *Homo* (i.e. Ceprano, Petralona and Dali).

The overall shape of the calvarium is similar in all vLCAs, but the projection on PC1 varies according to the position of the maximal cranial breadth (#9, euryon see Table C.3). vLCA3's euryon is positioned on the parietal, while the euryon is on the supramastoid crest (temporal) on the two other hypothetical ancestors. As a result, vLCA1 and 2 show the greatest affinity with the MP fossils Kabwe, Atapuerca SH5 and Omo II, which plot within the 95% confidence ellipsoid of the two chronological models, while vLCA3 is closer to the Neandertals, modern humans and the more recent MP fossils (i.e. LH18, Jebel Irhoud 1, Steinheim and Ehringsdorf H). Finally, it is interesting to note that the Eliye Spring specimen (KNM-ES 11693) is very similar to vLCA1 and 2 on PC1.

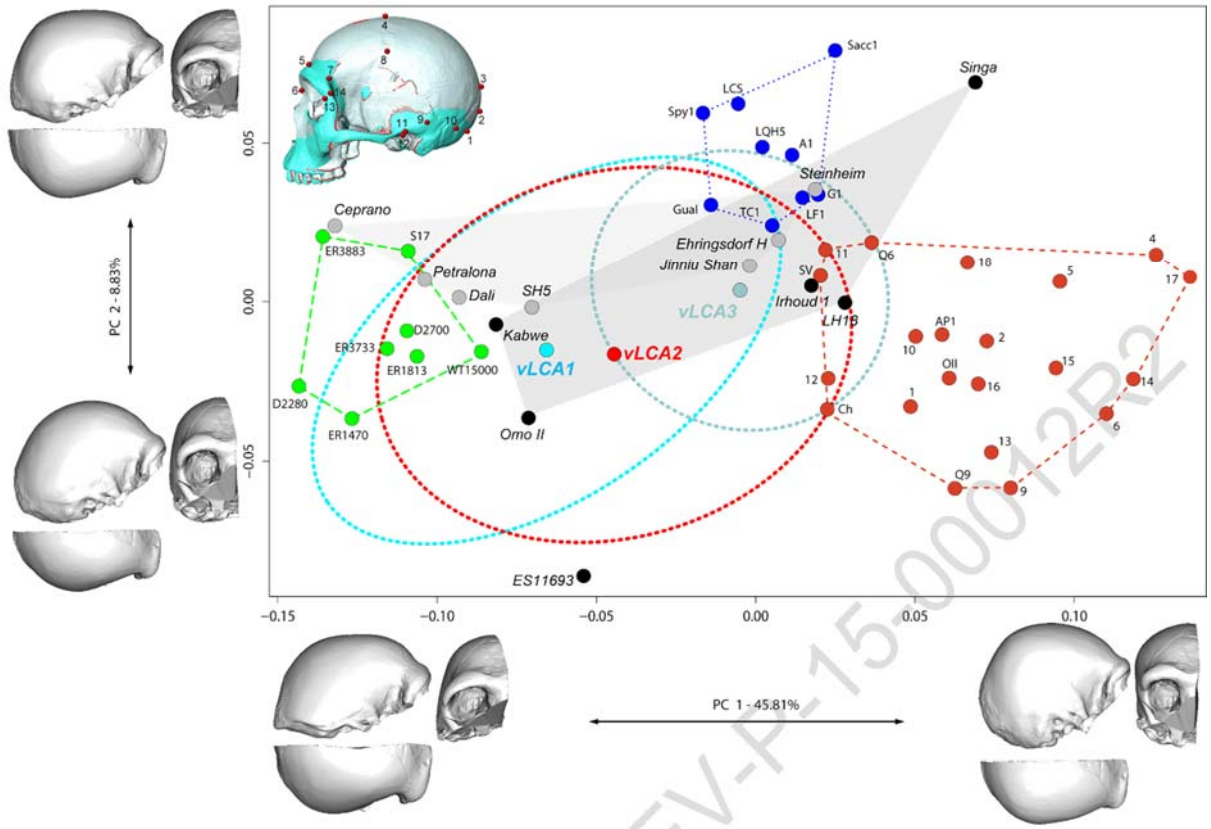

Figure 4. PC1 (45.81%) and PC2 (8.83%) of the PCA of the 14 landmarks of the calvarium. The three vLCAs are plotted along with a projection of the 95% confidence interval. Early *Homo* (green), Neandertals (blue) and modern humans (red) occupy distinct morphospaces on both PCs. The MP fossils (grey for Eurasians, black for Africans) form two clusters, one that approximates the Neandertal/modern human morphospaces and another closer to the early *Homo* specimens. The vLCAs plot in the middle of the chart along with some MP specimens: Omo II, Atapuerca SH5, Kabwe and to a lesser extent KNM-ES 11693.

Figure 5 shows the two first PCs (33.02% of the total variance) of the PCA based on the Procrustes residuals of the analysis of the upper face (Tables C.2 and C.3). On PC1, the modern humans present a flat mid and lower face with a flexed maxilla distinguishing them from the projecting Neandertal face. On PC2, the early *Homo* fossils show an elongated and rather flat face with a strong projection of the lower face. This morphology sets them apart from the rest of the sample. Contrary to the analysis of the calvarium, the MP sample shows a geographic trend, where most of the African fossils plot within or close to the modern human morphospace and most of the Eurasian ones plot closer to the Neandertal morphospace. Exceptions to this trend are the similarity of Bodo, Steinheim, Petralona and Kabwe with the three vLCAs. The facial morphology of the three hypothetical ancestors show similar affinities in all three cases. The vLCAs occupy a central position in the morphospace, being slightly more similar to Neandertals than to modern humans. It is worth noting that the upper face 95% confidence ellipsoids are small compared to those of the calvarium, which may be due to the reduced number of semi-landmarks used to describe the upper face (58 against 330 for the calvarium, see Fig. 2B and Material).

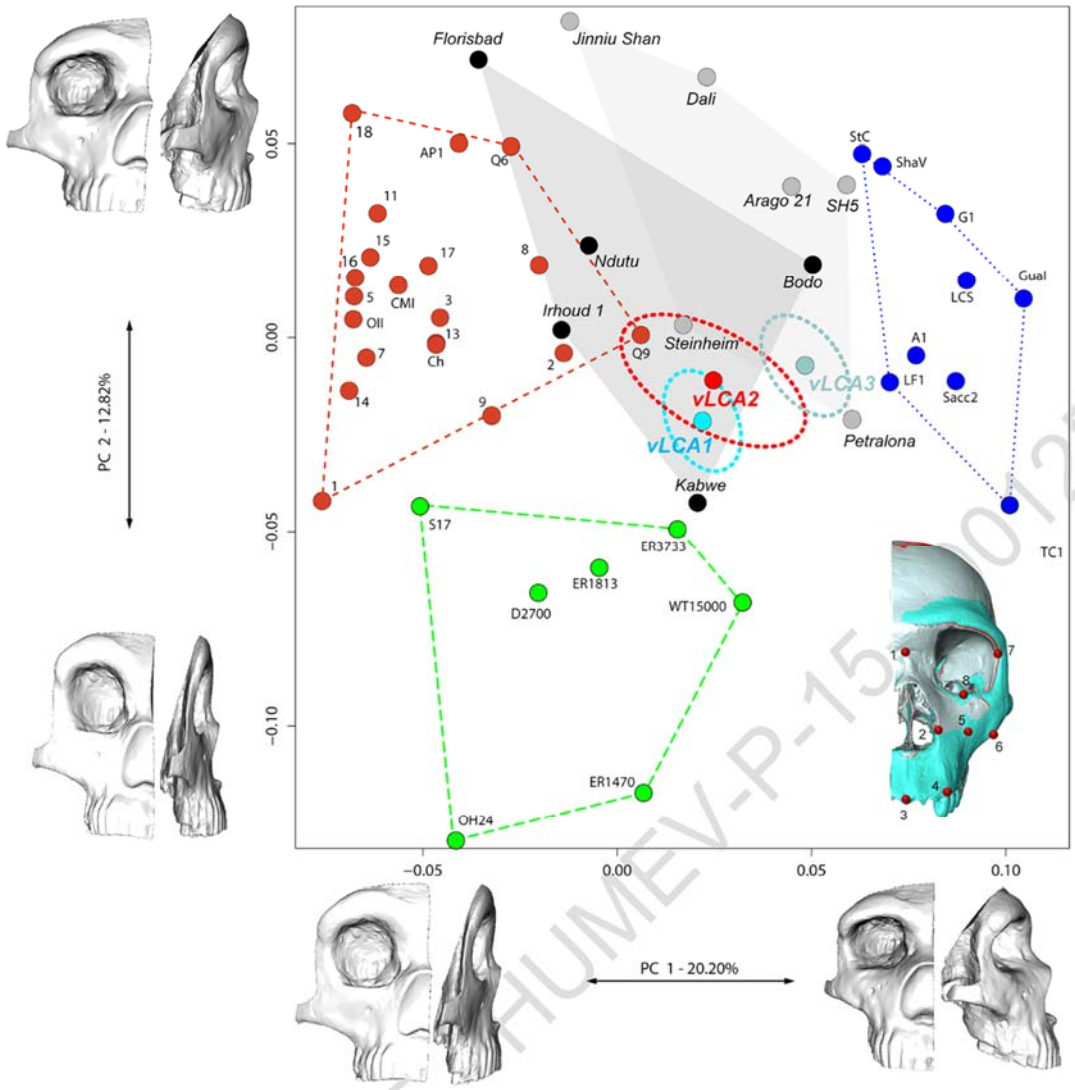

Figure 5. PC1 (20.20%) and PC2 (12.82%) of the PCA of the 8 landmarks of the upper face. The three vLCAs are plotted along with a projection of the 95% confidence interval. Early *Homo*, Neandertals and modern humans occupy distinct morphospaces on both PCs and the vLCAs plot in the middle of the chart along with some MP specimens: Bodo, Steinheim, Petralona and Kabwe.

Figure 6 depicts the MSTs based on the procrustes distances from the analysis of the calvarium. First, we note some variation in the cohesion of the three comparative groups. All the early *Homo* fossils are linked together, reflecting the relative morphological cohesion of the group, notwithstanding the complexity of early *Homo* systematics (Wood, 1993; Prat, 2004; Lordkipanidze et al., 2013). A similar situation is observed among modern humans, as they are all clustered together with the exception of a Holocene specimen (Romanian 1) and of Skhūl V and Qafzeh 6, while the Neandertals are separated in two groups linked by the MP fossil Steinheim. Concerning the MP specimens, Ceprano shows affinities to the early *Homo* KNM-ER 3733, which is surprising considering its morphological affinities to European MP specimens (Mounier et al., 2011), but may be partly accounted for by its heavily reconstructed cranial architecture (Ascenzi et al., 1996; Ascenzi et al., 2000; Clarke, 2000). LH18, Singa and Ehringsdorf H are directly linked to modern human specimens (respectively Saharan 1, Skhūl V and Qafzeh 6), while Steinheim is linked to both modern humans and Neandertals. Both LH18 and

Singa display strong morphological affinities with modern humans and could be attributed to *H. sapiens* (Bräuer, 2008; Spoor et al., 1998); however, the connection of Ehrinsgdorf H and Steinheim to modern humans is more surprising, as both specimens resemble the Neanderthals (Hublin, 1988; Condemi, 1992; Tattersall and Schwartz, 2006) notwithstanding numerous deformations in the case of Steinheim (Braun et al., 1998; Prossinger et al., 2003). Finally, Jebel Irhoud 1 is linked to a heterogenous cluster consisting of a Neandertal (Gibraltar 1), two modern humans (Skhūl V and Romanian 1) and to the MP fossil Jinniu Shan, which underlines Jebel Irhoud 1's mosaic morphology as well as its affinities to *H. sapiens* (Hublin, 2001).

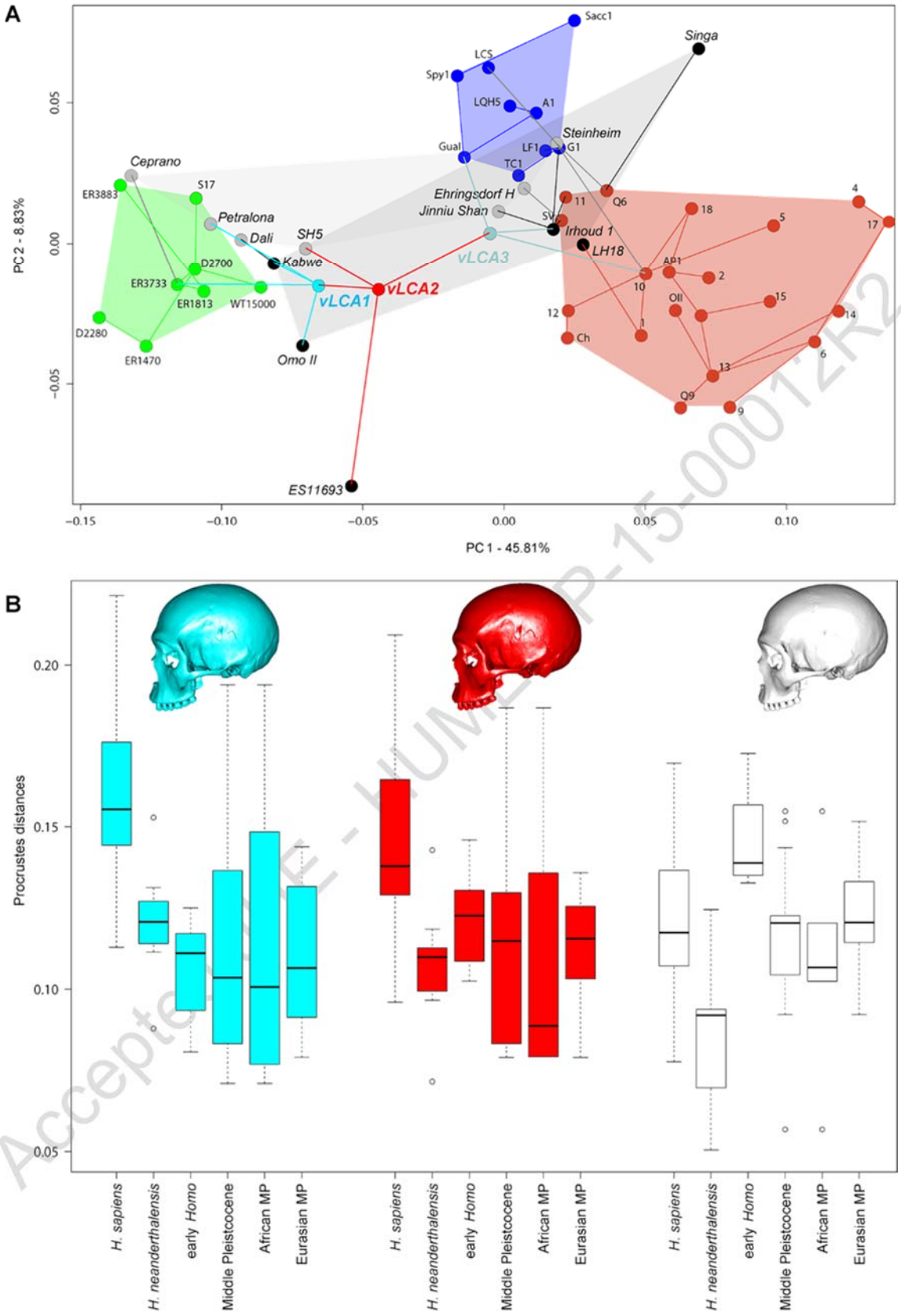

Figure 6. (A) Minimum spanning trees based on the procrustes distances for the analysis of the calvarium. Both vLCA1 and vLCA2 are mostly linked to MP fossils; vLCA3 is closer to Neandertals and modern humans. (B) Box-and-whisker plots of the Procrustes distances between the vLCAs (vLCA1 in blue, vLCA2 in red and vLCA3 in white) and each group of specimens used in the comparative analyses. Boxes are bounded by the upper and

lower quartiles and the bold line indicates the median. In median distance, both vLCA1 and vLCA2 show the most affinities to the African MP fossils, while vLCA3 is closest to the Neandertals.

Concerning the hypothetical ancestors, the vLCAs are statistically different from one another when considering their mean Procrustes distances to each comparative group (Anova: F=4.049, *p*=0.0194). The difference especially lies between vLCA1 and vLCA3 (Tukey multiple comparisons of means: *p*=0.0144). In terms of the median distances to each group (Fig. 6), they all share strong affinities with MP specimens. vLCA1 is directly linked to the African MP specimens Omo II and Kabwe and to the European fossil Petralona, as well as to the early *Homo* fossil KNM-ER 3733. The second vLCA is more closely related to the European Atapuerca SH5 calvarium and to the African MP fossil KNM-ES 11693. Both LCAs are linked to each other, while vLCA2 is connected to vLCA3 which, in turn, connects with the African MP Jebel Irhoud 1 specimen as well as with modern humans and the Neandertal Guattari I. The affinities of the vLCAs are further exemplified by their procrustes distances to the comparative sample (Fig. 6B and Table 3). vLCA1 is closer to the MP specimens (0.104), while vLCA2 and vLCA3 share more similarities with the Neandertals (respectively, 0.110 and 0.092). When looking at the MP geographical groups, all three vLCAs are closer to the African than the Eurasian sample, and in the case of vLCA2, it shares more affinities with the African MP specimens than with the Neandertals (respectively 0.089 and 0.110, see Figure 6B and Table 3). This pattern of similarity is further exemplified by the procrustes distances of the vLCAs when compared to the whole comparative sample. vLCA2 and vLCA3 are most similar to a Neandertal specimen (respectively Gibraltar 1 and Guattari I), but in the case of vLCA2 the Neandertal is followed by six MP fossils, while among the 10 closest individual to vLCA3 five are Neandertals (Table 4).

Table3. Procrustes distances of vLCAs to fossils.

	vLCA1	*vLCA2*	*vLCA3*		*vLCA1*	*vLCA2*	*vLCA3*
		Calvaria				**Upper face**	
Procrustes distances to Middle Pleistocene fossils							
Eurasia							
Atapuerca SH5	0.083	**0.079**	0.108	**Atapuerca SH5**	0.129	0.130	0.134
Ehringsdorf H	0.144	0.136	0.123	**Petralona**	**0.109**	**0.102**	0.151
Petralona	0.099	0.115	0.144	**Arago XXI**	0.119	0.108	**0.124**
Ceprano	0.106	0.121	0.152	**Steinheim**	0.133	0.136	0.144
Steinheim	0.127	0.116	**0.092**	**Dali**	0.131	0.127	0.150
Dali	**0.079**	0.092	0.121	**Jinniu Shan**	0.216	0.221	0.201
Jinniu Shan	0.137	0.130	0.120	**-**	**-**	-	**-**
Africa							
Kabwe	**0.071**	**0.079**	0.102	**Bodo**	0.107	0.111	**0.093**
Jebel Irhoud 1	0.098	0.083	**0.057**	**Kabwe**	0.126	0.128	0.137
LH18	0.148	0.136	0.109	**Jebel Irhoud 1**	**0.106**	**0.110**	0.138
KNM-ES 11693	0.104	0.094	0.120	**Florisbad**	0.141	0.135	0.160
Omo II	0.077	**0.079**	0.104	**Ndutu**	0.109	0.113	0.114
Singa	0.194	0.187	0.155	-	-	-	-
Median procrustes distances to groups							
H. sapiens	0.155	0.138	0.117	***H. sapiens***	**0.129**	0.128	0.157
H. neanderthalensis	0.121	**0.110**	**0.092**	***H. neanderthalensis***	0.139	0.144	**0.129**
Early *Homo*	0.111	0.123	0.139	**Early *Homo***	0.144	0.166	0.140
Middle Pleistocene	**0.104**	0.115	0.120	**Middle Pleistocene**	0.130	**0.127**	0.138
African MP	**0.101**	**0.089**	**0.107**	**African MP**	**0.118**	**0.113**	**0.137**
Eurasian MP	0.106	0.116	0.121	**Eurasian MP**	0.140	0.129	0.147

Pocrustes distances between each vLCA and the Middle Pleistocene fossil specimens and median procrustes distances between each vLCA and each group (*H. sapiens*, *H. neanderthalensis,* early *Homo,* Middle Pleistocene, African Middle Pleistocene and Eurasian Middle Pleistocene). The bold numbers indicate the shortest distance between each vLCA and the comparative sample.

Table 4. Procrustes distances between the vLCAs and the 20 closest specimens for the analyses of the calvarium and the upper face.

vLCA1		*vLCA2*		*vLCA3*	
		calvaria			
Kabwe	**0.071**	Guattari 1	0.071	Guattari 1	0.051
Omo II	**0.077**	**Atapuerca SH5**	**0.079**	**Jebel Irhoud 1**	**0.057**
Dali	**0.079**	**Omo II**	**0.079**	Gibraltar 1	0.063
KNM-ER 3733	0.080	**Kabwe**	**0.079**	Amud 1	0.070
Atapuerca SH5	**0.083**	**Jebel Irhoud 1**	**0.083**	La Ferrassie 1	0.073
Guattari 1	0.088	**Dali**	**0.092**	Skhul V	0.077
KNM-ER 1813	0.091	**KNM-ES 11693**	**0.094**	English2	0.084
D2700	0.096	Romanian2	0.096	Romanian2	0.087
Jebel Irhoud 1	**0.098**	Gibraltar 1	0.097	La Quina H5	0.092
Petralona	**0.099**	Skhul V	0.099	**Steinheim**	**0.092**
KNM-ES 11693	**0.104**	Amud 1	0.099	Spy 1	0.093
Ceprano	**0.106**	KNM-ER 3733	0.102	Tabun C1	0.094
KNM-ER 1470	0.110	KNM-ER 1813	0.106	La Chapelle-aux-Saints	0.100
Gibraltar 1	0.111	La Ferrassie 1	0.107	**Kabwe**	**0.102**
Sangiran 17	0.112	Spy 1	0.110	Qafzeh 6	0.104
KNM-WT 15000	0.113	D2700	0.111	**Omo II**	**0.104**
Skhul V	0.113	La Quina H5	0.112	Nigerian2	0.105
Amud 1	0.114	Tabun C1	0.113	Ohalo II	0.107
Romanian2	0.114	English2	0.115	**Atapuerca SH5**	**0.108**
Spy 1	0.119	**Petralona**	**0.115**	**LH18**	**0.109**
		upper face			
KNM-ER 1813	0.079	Qafzeh 9	0.083	**Bodo**	0.093
KNM-ER 3733	0.080	KNM-ER 3733	0.089	La Chapelle-aux -Saints	0.104
Qafzeh 9	0.086	Saharan2	0.091	Saccopastore 2	0.106
Saharan2	0.086	KNM-WT 15000	0.095	Saharan2	0.108
KNM-WT 15000	0.093	KNM-ER 1813	0.095	**Ndutu**	0.114
Saharan3	0.093	Saharan3	0.096	KNM-ER 1813	0.120
Chinese1	0.105	Amud 1	0.100	Chinese1	0.123
Jebel Irhoud 1	0.106	**Petralona**	0.102	**Arago 21**	0.124
Bodo	0.107	**Arago 21**	0.108	Qafzeh 9	0.125
Ndutu	0.109	Chinese1	0.109	French1	0.125
Petralona	0.109	**Jebel Irhoud 1**	0.110	Guattari I	0.126
Amud 1	0.110	**Bodo**	0.111	Amud 1	0.128
La Chapelle-aux -Saints	0.114	**Ndutu**	0.113	Saharan3	0.128
Chinese2	0.116	Indonesian2	0.114	Gibraltar 1	0.129
Indonesian1	0.117	Chinese2	0.114	Tabun C1	0.130
French1	0.118	French1	0.114	KNM-ER 3733	0.130
Arago 21	0.119	La Chapelle-aux -Saints	0.114	**Atapuerca SH5**	0.134
Indonesian2	0.120	English1	0.115	**Kabwe**	0.137
English1	0.121	Indonesian1	0.118	**Jebel Irhoud 1**	0.138
Cro-Magnon I	0.122	Gibraltar 1	0.124	KNM-WT 15000	0.139

The Middle Pleistocene fossils are in bold. The procrustes distances to all the specimens of the comparative sample are available in Tables C.4 and C.5.

The network depicted by the MSTs for the analysis of the upper face is more complicated (Fig. 7). First, the early *Homo* specimens present very poor cohesion; only four of the seven fossils show intra-group links (D2700 with KNM-WT 15000 and KNM-ER 1813 with KNM-ER1470) and the Sangiran 17 face shows affinities with the modern human MST. These results reflect the heterogeneity in the facial morphology of this group and, in the case of Sangiran 17, its peculiar preservation state (Rightmire, 1990). Similarly, the Neandertals show two unconnected minimum trees and three specimens are not

linked with either of those (St Césaire, La Ferrassie 1 and Tabūn C1). The relative isolation of Tabūn can be explained by the less derived morphology generally observed among Eastern Neandertals (Trinkaus, 1983; Condemi, 1991) and by its poorly preserved upper face from which three landmarks were estimated (#5, infra-orbital; #6, zygo-maxillar anterior; #8 zygo-orbital, Table 4). The modern human sample shows greater cohesion, as only two specimens (English 1 and Qafzeh 9) remain out of the main minimum tree. With the exception of Steinheim, which is linked to Ndutu, none of the MP specimens are connected to other MP fossils. Florisbad, Ndutu, Kabwe and Jinniu Shan connect with the modern human MST, Dali shows affinities with Qafzeh 9 and its singular morphology (Vandermeersch, 1981), as does Jebel Irhoud 1 which, surprisingly, also connects with the highly distorted early *Homo* specimen OH24 (Leakey et al., 1971). The morphological similarities between the African MP fossils Jebel Irhoud 1, Ndutu and Florisbad and modern humans has been suggested before (Clarke, 1990; Hublin, 2001; Bräuer, 2008; Mounier, 2009) and are thus not surprising. While more controversial for the Asian fossils Dali and Jinniu Shan, such affinities have also been noted before (Mounier, 2009, 2011; Pope, 1992). The other specimens Arago 21, Atapuerca SH5 and Petralona are linked to the Neandertals, which is consistent with the presence of features considered Neandertal apomorphies among the MP European fossil record (Condemi, 1989; Dean et al., 1998).

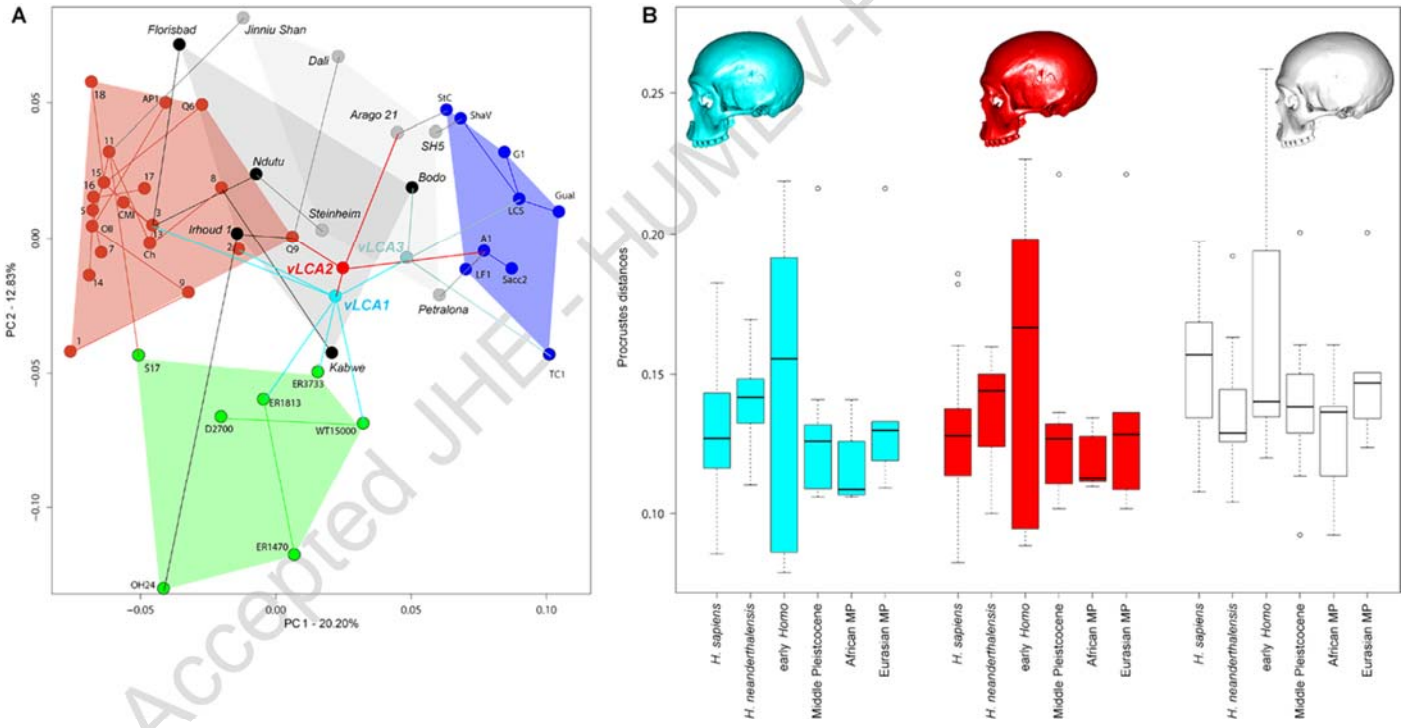

Figure 7. (A) Minimum spanning trees based on the Procrustes distances for the analysis of the upper face. vLCA1 is not directly linked to any of the MP fossils, vLCA2 and vLCA3 are only linked to one MP fossil, respectively Arago 21 and Bodo. (B) Box-and-whisker plots of Procrustes distances between the vLCAs (vLCA1 in blue, vLCA2 in red and vLCA3 in white) and each group of specimens. Boxes are bounded by the upper and lower quartiles and the bold line indicates the median. In median distance, both vLCA1 and vLCA2 show the most affinities to the African MP fossils, while vLCA3 is closest to the Neandertals.

As for the analysis of the calvarium, the analysis of the upper face of the three hypothetical ancestors show that they are statistically different from one another when considering their mean Procrustes distances to each comparative group (Anova: F=3.518, *p*=0.0324). The difference especially lies between vLCA1 and vLCA3 (Tukey multiple comparisons of means: *p*=0.0547624), but they show few connections with the MP specimens. vLCA1 is linked with early *Homo* fossils (KNM-ER 3733, KNM-ER 1813 and KNM-WT 15000), with the modern human tree cluster and with the two other virtual ancestors. vLCA2 is connected to Qafzeh 9 on the *H. sapiens* side and to Amud 1 on the Neandertal side; it is also similar to the European MP Arago 21. vLCA3 is connected to the Neandertals (Tabun C1 and La Chapelle-aux-Saints), but also shows similarities to Bodo. Looking at the Procrustes distances of the virtual ancestors (Fig. 7B and Table 3), the picture is less complicated. vLCA1 shares more affinities with modern humans (0.129), vLCA2 is closest to MP fossils (0.127) and vLCA3 is more similar to the Neandertals (0.129). As we observed for the analysis of the calvarium, all three vLCAs are closer to Africans (respectiveley, 0.118, 0.113 and 0.139) when the MP fossils are separated into geographical groups. vLCA1 shares more similarities with the African MP fossils than with modern humans (respectively, 0.118 and 0.129). However, when looking at the similarity of each of the three vLCAs to each fossil of the comparative samples (Table 4), we can see that, with the exception of vLCA3 (most similar to Bodo), there are no MP fossils in the closest five specimens to vLCA1 and vLCA2.

Discussion and conclusions

These analyses show that the vLCAs of modern humans and Neandertals closely resemble real MP fossil hominins, clearly placing the ancestral morphology within a Middle Pleistocene hypodigm. The three chronological models tested (Fig. 2) show a similar morphological pattern that possesses both derived and plesiomorphic traits (see above, Fig. 3 and Appendix B).

When comparing the morphological differences between the three models, they follow a chronological pattern as expected under a Brownian motion model, where the ancestral state is a weighted average of the tip states, depending on the branch length. From vLCA1 (1 Ma common ancestry) to vLCA2 (0.7 Ma common ancestry) to vLCA3 (0.4 Ma common ancestry), we note 1) a retraction of the lower face which projects strongly in vLCA1; 2) an increase in mid-facial projection, so that the mid-facial projection of vLCA3 resembles that of Neandertals; 3) a slight increase in the pneumatisation of the maxilla; 4) a slight reduction of the supra-orbital torus accompanied by a slight increase in glabella size; 5) an increase in basicranial flexion as well as a decrease in basicranial length; and 6) an increase in the globularity of the calvarium.

In terms of morphological affinities of the different models with the extant MP fossil record, it is of interest to note that vLCA3 is the most distant from the MP fossil sample (Tables 3 and 4), both in terms of the morphology of the calvarium and upper face. It shares strong affinities with the Neandertals which is expected as Neandertals are, chronologically, closest to this virtual fossil than any other comparative group. Nevertheless, its affinity to one of the closest descendant groups separates vLCA3 from the other two vLCAs. vLCA2 shows the highest affinities with the actual MP fossil record based on both the calvarium and the face, while vLCA1 is intermediate and shows strong affinities with early *Homo* on the basis of the calvarium (Tables 3 and 4). In more detail, vLCA1's

morphology is closest to Kabwe (calvarium) and Jebel Irhoud (face); vLCA2 is more similar to Atapuerca SH5, Kabwe and Omo II (calvarium) and Petralona (face); and vLCA3 is closer to Jebel Irhoud 1 (calvarium) and Bodo (face) (Table 4). It is interesting to note that morphological affinities of the calvaria and the upper faces of the vLCAs show different patterns, and indeed the MST on the facial morphology as captured by the landmarks used in this study does not reconstruct most of the main groups included in the comparative sample. The morphology of the face is considered to be more susceptible to evolutionary change: it has been described as accumulating new derived features faster than the more conservative calvarium (see the 'Accretion Model', Condemi, 1989; Dean et al., 1998), as well as to reflect climatic adaptations (Harvati and Weaver, 2006). Nevertheless, vLCA3 shared morphological affinities with the calvarium of Jebel Irhoud 1 and the face of Bodo might appear strange considering the estimated chronology of both specimens - respectively *ca.* 130ka (Grün and Stringer, 1991) and *ca.* 600ka (Clark et al., 1994) - and the much more derived morphology of Jebel Irhoud 1 (Hublin, 2001; Mounier, 2011). This peculiar affinity pattern must be discussed within the framework of overall strong morphological similarity of vLCA3 with the Neandertals as shown by the mean and individual procrustes distances (Tables 3, 4, C.4 and C.5): both Jebel Irhoud 1 (Ennouchi, 1963) and Bodo (Mounier, 2012) have been described as presenting affinities with the Neandertals, even though they do not share apomorphies with *H. neanderthalensis* (Hublin, 1992; Mounier, 2011; Rightmire, 1996). On the contrary, the general morphological pattern of vLCA1 and vLCA2 seems more accurate within a framework of an Afro-European Middle Pleistocene population as the ancestor of modern humans and Neandertals (Mounier, 2009; Rightmire, 1998).

Having assessed the morphological patterns and affinities of the three vLCAs, what can this tell us in term of the phylogenetic history of *H. sapiens* and *H. neanderthalensis*? The models are hypotheses themselves and raise new questions about the signal recorded by different lines of evidence as well as, within the realm of morphology, the signal recorded by different elements. Model 1, with a common ancestry in the late Lower Pleistocene (see, Gómez-Robles et al., 2013; Gómez-Robles et al., 2015), is theoretically the least supported hypothesis as it is inconsistent with the increasing palaeogenetic evidence that suggests a Middle Pleistocene age for the common ancestor of Neandertals and modern humans. The hypothetical ancestor representing this early split between modern humans and Neandertals captures an early Middle Pleistocene morphology both in the face and calvarium. While not the best model in terms of distance to the descendant forms and similarities between younger African and European fossils, this deeper ancestry for the two regional lineages remains morphologically possible. It is interesting to note that, in the context of the different signals reflected in different anatomical elements, such deep ancestry has been recently supported by analyses of dental morphology (Gómez-Robles et al., 2015). Additionally, such a model is difficult to test considering the scarcity of the fossil record for this time period (i.e. ~1 Ma).

Models 2 (early Middle Pleistocene) and 3 (mid-Middle Pleistocene) would both be consistent with the palaeogenetic evidence. However, as we have demonstrated, the morphological affinity of vLCA3 is clearly with the Neandertals. This means that given the morphology of modern humans and Neandertals and assuming equal rates of evolution along both lineages, if their LCA was recent it would have already looked 'Neandertal' rather than like known Middle Pleistocene specimens. While again, this cannot be excluded, it is an unlikely LCA for both *H. sapiens* and *H. neanderthalensis* (unless the

sapiens lineage were significantly derived in relation to the LCA), and inconsistent with the range of variation of the available small number of mid Middle Pleistocene fossil specimens. vLCA3 was estimated at 400 ka; a MP fossil sample encompassing that period would include in Africa a group of fossils of controversial age, such as Kabwe, Ndutu and Eliye Springs, and in Europe the fossils of Atapuerca, Arago, Ceprano and possibly Petralona. vLCA3 shows no affinity to any of these specimens, either individually or as groups. It could be argued that, rather than showing similarities to contemporary remains, the vLCA should resemble a more recent population, to which it was presumably an ancestor. Late Middle Pleistocene fossils in Africa are few, including Jebel Irhoud, Ngaloba, Omo Kibish and Florisbad, and in Europe, including Steinheim and Ehringsdorf. This group of African fossils has been grouped in the taxon *H. helmei* (McBrearty and Brooks, 2000), which for others also includes the contemporary Eurasian material (Foley and Lahr, 1997; Lahr and Foley, 1998), representing either a chronospecies within an African evolving lineage or the species ancestral to modern humans and Neandertals respectively. vLCA3, with its affinities to Neandertals does not support either of these hypotheses. However, when compared only to a MP sample, the closest distance found to vLCA3 was to Jebel Irhoud, pointing to the complex pattern of derived and conservative features across the cranium. On the contrary, the morphology of vLCA2 corresponds in many instances to a diagnosis of *H. heidelbergensis* s.l. (Mounier, 2009), and seems to offer support for an Afro-European ancestral taxon (Rightmire, 2008; Mounier et al., 2009; Stringer, 2012). However, despite the discrepancies between the calvarium and the upper face, our results further show that the vLCA (whether vLCA1 or vLCA2) has a greater affinity to African than to European MP specimens, with some aspects of its morphology approximating both late MP African specimens (a well-developed supraorbital region but a small glabella as in Florisbad and LH 18) and earlier ones (long, projecting, non-pneumatised face as in Bodo, incipient occipital bun and supra-iniac fossa as in Kabwe). This would suggest that the root of this ancestral population is likely to have been in Africa, as has been recently argued on dental evidence (Gómez-Robles et al., 2013) and through a cladistics study of MP fossil morphology (Mounier and Caparros, 2015). Nevertheless, this does not fully answer the question of the chronology. The most coherent morphological pattern, yet undiscovered in a single fossil specimen, is vLCA2 with an early Middle Pleistocene divergence between the modern human and Neandertal lineages.

Recent aDNA results, highlighting interbreeding across regional Pleistocene hominin populations and revealing a new Eurasian population (Denisovans), add more complexity to the systematics of later *Homo.* If we consider vLCA2 as the best candidate for the common Neandertal-modern ancestry, our results are consistent with the second of the phylogenetic hypotheses tested here (Model 2, Fig. 1): vLCA2 is closer to Neandertals (at least on the more conservative calvarium), but is also more likely to have lived in Africa than in Europe. This implies that the ancestral population of *H. sapiens* and *H. neanderthalensis* may have been African, and that subsequent modern human populations have undergone a higher rate of morphological change compared to Neandertals. This is consistent with recent phylogenies being proposed on the basis of aDNA (Prüfer et al., 2014) and with the prediction based on genomic data made by Endicott et al. (2010). Recent analyses by Weaver and colleagues (Weaver et al., 2007, 2008) showed that a model of genetic drift was more compatible with the morphological differences between modern humans and Neandertals than natural selection. The possibility of a higher rate of morphological change in the modern human lineage suggested by our results would be consistent with periods of major demographic change and genetic drift, as shown by

numerous genetic analyses. Despite the fact that our vLCAs support an African origin for the common ancestor of modern humans and Neandertals, it remains the case that numerous morphological features, especially on the face, point to affinities between MP European fossils and Neandertals to the exclusion of modern humans. Such similarities could represent the result of strong convergence in facial morphology (Lahr and Foley, 1998). An alternative explanation would be to consider a model in which the speciation of modern humans and Neandertals could have emerged through a complex web of contacts between geographically separated populations that were variously isolated within refugia during the early Middle Pleistocene in, and probably out of, Africa (Mounier and Caparros, 2015).

Further genomic studies will help clarify some of these issues, but only a greater number of fossils – real and virtual – will allow us to interpret the pattern and process of phenotypic change in later *Homo.*

Acknowledgments

This study was partially funded by the Fyssen Foundation, and an Advanced ERC Award (IN-AFRICA Project). For permission to study specimens in their care we thank directors and curators of the following institutions: Musée de l'Homme (Paris, France); Institut de Paléontologie Humaine (Paris, France); Staatliches Museum für Naturkunde (Stuttgart, Germany); Aristotle University of Thessaloniki (Thessaloniki, Greece); Soprintendenza Archeologia del Lazio, Servizio di Antropologia (Rome, Italy); Museo di Antropologia G. Sergi (Sapienza Università di Roma, Italy); Museo preistorico-etonografico ''L. Pigorini'' (Rome, Italy); National Museums of Kenya (Nairobi, Kenya); National Museum (Bloemfontein, Republic of South Africa); Natural History Museum (London, UK); Duckworth Collection (Cambridge, UK). We thank F. Lahr and F. Rivera for assistance with CT-scanning and E. Delson, R. Foley, L. Puymerail and A. Froment for help and ideas. Finally, we thank M. Plavcan, D. Polly, the Associate Editor and two anonymous reviewers for valuable comments and criticisms of earlier drafts which contributed to the improvement of this study.

References

Adams, D.C., Otárola-Castillo, E., 2013. geomorph: an r package for the collection and analysis of geometric morphometric shape data. Met. Ecol. Evol. 4, 393-399.

Arsuaga, J.L., Martínez, I., Gracia, A., Lorenzo, C., 1997. The Sima de los Huesos crania (Sierra de Atapuerca, Spain). A comparative study. J. Hum. Evol. 33, 219-281.

Ascenzi, A., Biddittu, I., Cassoli, P.F., Segre, A.G., Segre-Naldini, E., 1996. A calvarium of late *Homo erectus* from Ceprano, Italy. J. Hum. Evol. 31, 429-423.

Ascenzi, A., F., M., Manzi, G., Segre, A.G., Segre Naldini, E., 2000. A re-appraisal of Ceprano calvaria affinities with *Homo erectus*, after the new reconstruction. J. Hum. Evol. 39, 443-450.

Baab, K.L., 2008. The taxonomic implications of cranial shape variation in *Homo erectus*. J. Hum. Evol. 54, 827-847.

Bar-Yosef, O., 1998. Chronology of the Middle Paleolithic of the Levant. In: Akazawa, T., Aoki, K., Bar-Yosef, O. (Eds.), Neandertals and modern humans in Western Asia. Plenum, New York, pp. 39-56.

Baum, D., 1992. Phylogenetic species concepts. Trends Ecol. Evol. 7, 1-2.

Beerli, P., Edwards, S.V., 2002. When did Neanderthals and modern humans diverge? Evol. Anthropol. 11, 60-63.

Bermúdez de Castro, J.M., Arsuaga, J.L., Carbonell, E., Rosas, A., Martínez, I., Mosquera, M., 1997. A hominid from the Lower Pleistocene of Atapuerca, Spain: possible ancestor to Neandertals and modern humans. Science. 276, 1392–1395.

Bermúdez de Castro, J.M., Martinón-Torres, M., Carbonell, E., Sarmiento, S., Rosas, A., van der Made, J., Lozano, M., 2004. The Atapuerca sites and their contribution to the knowledge of human evolution in Europe. Evol. Anthropol. 13, 25-41.

Blackwell, B., Montoya, A.C., Bisson, M.S., Bliscksteín, J.I.B., Skinner, A.R., Beelitz, P., 2007. ESR dating bovid teeth from the Neanderthal layer at La Ferrassie, France. Geo. Soc. Am. 39, 548.

Bookstein, F.L., 1989. Principal warps: thin-plate splines and the decomposition of deformations. IEEE Trans. Pattern Anal. Mach. Intell. 11, 567-585.

Bookstein, F.L., 1991. Morphometric Tools for Landmark Data: Geometry and Biology. Cambridge University Press, Cambridge.

Bookstein, F.L., 1997. Landmark methods for forms without landmarks: morphometrics of group differences in outline shape. Med. Image. Anal. 1, 225-243.

Boule, M., 1911-1913. L'Homme fossile de La Chapelle-aux-Saints. Annls. Paléonto. (Vert.) 6, 7, 8, 109-172, 105-192, 101-162.

Bräuer, G., 2008. The origin of modern anatomy: By speciation or intraspecific evolution? Evol. Anthropol. 17, 22-37.

Braun, M., Hublin, J.J., Bouchet, P., 1998. New reconstruction of the Middle Pleistocene skull of Steinheim (Baden-Würtemberg, Germany). Am. J. Phys. Anthropol. suppl 26, 113.

Bricker, H., Mellars, P., 1987. Datations 14C de l'Abri Pataud (Les Eyzies, Dordogne) par le procédé "accélérateur-spectromètre de masse". L'Anthropologie. 91, 227-234.

Brown, F.H., McDougall, I., 1993. Geologic setting and age. In: Walker, A.C., Leakey, R.E.F. (Eds.), The Nariokotome *Homo erectus* skeleton. Springer-Verlag, Berlin, pp. 9-20.

Bruner, E., Manzi, G., 2006. Saccopastore 1: the earliest Neanderthal? A new look at an old cranium. In: Harvati, K., Harrison, T. (Eds.), Neanderthals Revisited. Springer, New York, pp. 23-36.

Carbonell, E., Bermúdez de Castro, J.M., Arsuaga, J.L., Allue, E., Bastir, M., Benito, A., Cáceres, I., Canals, T., Díez, J.C., van der Made, J., Mosquera, M., Ollé, A., Pérez-González, A., Rodríguez, J., Rodríguez, X.P., Rosas, A., Rosell,

J., Sala, R., Vallverdú, J., Vergés, J.M., 2005. An Early Pleistocene hominin mandible from Atapuerca-TD6, Spain. Proc. Natl. Acad. Sci. 102, 5674–5678.

Carbonell, E., Bermúdez de Castro, J.M., Arsuaga, J.L., Rosas, A., Cuenca-Besccos, G., Sala, R., Mosquera, M., Rodriguez, X.P., 1995. Lower Pleistocene hominids and artifacts from Atapuerca-TD6 (Spain). Science. 269, 826-830.

Carbonell, E., Bermúdez de Castro, J.M., Parés, J.M., Pérez-González, A., Cuenca-Bescós, G., Ollé, A., Mosquera, M., Huguet, R., van der Made, J., Rosas, A., Sala, R., Vallverdú, J., García, N., Granger, D.E., Martinón-Torres, M., Rodríguez, X.P., Stock, G.M., Vergès, J.M., Allué, E., Burjachs, F., Cáceres, I., Canals, A., Benito, A., Díez, C., Lozano, M., Mateos, A., Navazo, M., Rodríguez, J., Rosell, J., Arsuaga, J.L., 2008. The first hominin of Europe. Nature. 452, 465-469.

Carmi, I., Segal, D., 1992. Rehovot radiocarbon measurements IV. Radiocarbon. 34, 115-132.

Clark, J.D., de Heinzelin, J., Schick, K.D., Hart, W.K., White, T.D., WoldeGabriel, G., Walter, R.C., Suwa, G., Asfaw, B., Vrba, E.S., Haile-Selassie, Y., 1994. African *Homo erectus* : old radiometric ages and young oldowan assemblages in the Middle Awash Valley, Ethiopia. Science. 264, 1907-1910.

Clarke, R.J., 1990. The Ndutu cranium and the origin of *Homo sapiens*. J. Hum. Evol. 19, 699-736.

Clarke, R.J., 2000. A corrected reconstruction and interpretation of the *Homo erectus* calvaria from Ceprano, Italy. J. Hum. Evol. 39, 433-442.

Condemi, S., 1989. Décalage dans l'apparition des traits néanderthaliens sur le crâne cérébral chez les fossiles du Riss-Würm. In: Giacobini, G. (Ed.), Hominidae. Jaca Book, Milano, pp. 357-362.

Condemi, S., 1991. Some considerations concerning Neandertal features and the presence of Neandertals in the Near East. Rivista di Antropologia (Roma). LXIX, 27-38.

Condemi, S., 1992. Les Hommes Fossiles de Saccopastore et leurs Relations Phylogénétiques. CNRS Editions, Paris.

de Lumley, H., Lordkipanidze, D., Féraud, G., Garcia, T., Perrenoud, C., Falguères, C., Gagnepain, J., Saos, T., Voinchet, P., 2002. Datation par la méthode 40Ar/39Ar de la couche de cendres volcaniques (couche VI) de Dmanissi (Géorgie) qui a livré des restes d'hominidés fossiles de 1,81 Ma. Comptes Rendus Palevol. 1, 181-189.

Dean, D., Hublin, J.-J., Holloway, R., Ziegler, R., 1998. On the phylogenetic position of the pre-Neandertal specimen from Reilingen, Germany. J. Hum. Evol. 34, 485–508.

Dutour, O., 1989. Hommes Fossiles du Sahara. Peuplements holocènes du Mali septentrional. Editions du CNRS, Paris.

Dutour, O., 1994. L'hypogée de Loisy en brie (Marne); lieu dit la Goutte d'Or. Préhistoire et Protohistoire en Champagnes Ardennes. 18, 63-64.

Edwards, A.W.F., Cavalli-Sforza, L.L., 1964. Reconstruction of evolutionary trees. In: Heywood, V.H., McNeill, J. (Eds.), Reconstruction of Evolutionary Trees. Systematic Association, London, pp. 67-76.

Endicott, P., Ho, S.Y.W., Stringer, C., 2010. Using genetic evidence to evaluate four palaeoanthropological hypotheses for the timing of Neanderthal and modern human origins. J. Hum. Evol. 59, 87-95.

Ennouchi, E., 1963. Les Néanderthaliens du Jebel Irhoud (Maroc). C R Acad Sci Paris 256, 2459-2460.

Excoffier, L., Smouse, P.E., 1994. Using allele frequencies and geographic subdivision to reconstruct gene trees within a species: molecular variance parsimony. Genetics 136, 343-359.

Fabre, V., Condemi, S., Degioanni, A., 2009. Genetic evidence of geographical groups among neanderthals. PLoS ONE. 4, e5151.

Feibel, C.S., Lepre, C.J., Quinn, R.L., 2009. Stratigraphy, correlation, and age estimates for fossils from Area 123, Koobi Fora. J. Hum. Evol. 57, 112-122.

Felsenstein, J., 1981. Evolutionary trees from DNA sequences: a maximum likelihood approach. J. Mol. Evol. 17, 368-376.

Felsenstein, J., 1985. Phylogenies and the comparative method. Am. Nat. 125, 1-15.

Felsenstein, J., 1988. Phylogenies and quantitative characters. Ann. Rev. Ecol. Syst. 19, 445-471.

Foley, R.A., Lahr, M.M., 1997. Mode 3 technologies and the evolution of modern humans. Cambridge Archaeol. J. 7 3-36.

Fu, Q., Li, H., Moorjani, P., Jay, F., Slepchenko, S.M., Bondarev, A.A., Johnson, P.L.F., Aximu-Petri, A., Prüfer, K., de Filippo, C., Meyer, M., Zwyns, N., Salazar-Garcia, D.C., Kuzmin, Y.V., Keates, S.G., Kosintsev, P.A., Razhev, D.I., Richards, M.P., Peristov, N.V., Lachmann, M., Douka, K., Higham, T.F.G., Slatkin, M., Hublin, J.-J., Reich, D., Kelso, J., Viola, T.B., Paabo, S., 2014. Genome sequence of a 45,000-year-old modern human from western Siberia. Nature. 514, 445-449.

Fu, Q., Mittnik, A., Johnson, P.L.F., Bos, K., Lari, M., Bollongino, R., Sun, C., Giemsch, L., Schmitz, R., Burger, J., Ronchitelli, A.M., Martini, F., Cremonesi, R.G., Svoboda, J., Bauer, P., Caramelli, D., Castellano, S., Reich, D., Pääbo, S., Krause, J., 2013. A revised timescale for human evolution based on ancient mitochondrial genomes. Curr. Biol. 23, 553-559.

Gathogo, P.N., Brown, F.H., 2006. Revised stratigraphy of Area 123, Koobi Fora, Kenya, and new age estimates of its fossil mammals, including hominins. J. Hum. Evol. 51, 471-479.

Gómez-Robles, A., Bermúdez de Castro, J.M., Martinón-Torres, M., Prado-Simón, L., Arsuaga, J.L., 2015. A geometric morphometric analysis of hominin lower molars: evolutionary implications and overview of postcanine dental variation. J. Hum. Evol. 82, 34-50.

Gómez-Robles, A., Bermúdez de Castro, J.M., Arsuaga, J.-L., Carbonell, E., Polly, P.D., 2013. No known hominin species matches the expected dental morphology of the last common ancestor of Neanderthals and modern humans. Proc. Natl. Acad. Sci. 110, 18196-18201.

Gower, J.C., 1975. Generalised Procrustes analysis. Psychometrika. 40, 33-50.

Groves, C., Lahr, M.M., 1994. A bush not a ladder: Speciation and replacement in human evolution. Perspect. Hum. Biol. 4, 1-11.

Grün, R., Stringer, C., McDermott, F., Nathan, R., Porat, N., Robertson, S., Taylor, L., Mortimer, G., Eggins, S., McCulloch, M., 2005. U-series and ESR analyses of bones and teeth relating to the human burials from Skhūl. J. Hum. Evol. 49, 316-334.

Grün, R., Stringer, C.B., 1991. ESR dating and the evolution of modern humans. Archaeometry. 33, 153-199.

Grün, R., Stringer, C.B., 2000. Tabun revisited: Revised ER chronology and new ESR and U-series analyses of dental material from Tabun C1. J. Hum. Evol. 39, 601-612.

Gunz, P., 2005. Statistical and geometric reconstruction of hominid crania: recon-structing australopithecine ontogeny. Ph.D. Dissertation, University of Vienna.

Gunz, P., Mitterocker, P., Bookstein, F., 2005. Semilandmarks in three dimensions. In: Slice, D.E. (Ed.), Modern Morphometrics in Physical Anthropology. Kluwer Academic, Plenum Publishers, New York, pp. 73-98.

Gunz, P., Mitteroecker, P., 2013. Semilandmarks: a method for quantifying curves and surfaces. Hystrix. 24, 103-109.

Harvati, K., Weaver, T.D., 2006. Human cranial anatomy and the differential preservation of population history and climate signatures. Anat. Rec. 288A, 1225-1233.

Henry-Gambier, D., 2002. Les fossiles de Cro-Magnon (Les Eyzies-de-Tayac, Dordogne) : nouvelles données sur leur position chronologique et leur attribution culturelle. Bull. Mém. Soc. Anthropol. Paris. 14, 89-112.

Hublin, J.-J., 1988. Les plus anciens représentants de la lignée prénéandertalienne. In: Trinkaus, E. (Ed.), L'Homme de Néandertal. Volume 3, l'anatomie, ERAUL ed. Université de Liège, Liège, pp. 81-94.

Hublin, J.J., 1992. Recent human evolution in northwestern Africa. Philos. Trans. R. Soc. 337, 185-191.

Hublin, J.-J., 2001. Northwestern Africa and Middle Pleistocene hominids and their bearing on the emergence of *Homo sapiens*. In: Barham, L., Robson-Brown, K. (Eds.), Human Roots: Africa and Asia in the Middle Pleistocene, CHERUB ed. Western Academic & Specialist Press Ltd, Bristol, pp. 99-121.

Hublin, J.-J., 2009. The origin of Neandertals. Proc. Natl. Acad. Sci. 106, 16022-16027.

Krause, J., Fu, Q., Good, J.M., Viola, B., Shunkov, M.V., Derevianko, A.P., Pääbo, S., 2010. The complete mitochondrial DNA genome of an unknown hominin from southern Siberia. Nature. 464, 894-897.

Lahr, M.M., Foley, R., 2001. Mode 3, *Homo helmei*, and the pattern of human evolution in the Middle Pleistocene.. In: Barham, L., Robson-Brown, K. (Eds.), Human Roots: Africa and Asia in the Middle Pleistocene. Western Academic & Specialist Press, Bristol, pp. 23-39.

Lahr, M.M., Foley, R.A., 1998. Towards a theory of modern human origins: Geography, demography, and diversity in recent human evolution. Yearb. Phys. Anthropol. 41, 137-176.

Larick, R., Ciochon, R.L., Zaim, Y., Suminto, Sudijono, Rizal, Y., Aziz, F., Reagan, M., Heizler, M., 2001. Early Pleistocene 40Ar/39Ar ages for Bapang Formation hominins, Central Java, Indonesia. Proc. Natl. Acad. Sci. 98, 4866-4871.

Leakey, M.D., Clarke, R.J., Leakey, L.S.B., 1971. New Hominid Skull from Bed I, Olduvai Gorge, Tanzania. Nature 232, 308-312.

Leakey, M.G., Spoor, F., Dean, M.C., Feibel, C.S., Anton, S.C., Kiarie, C., Leakey, L.N., 2012. New fossils from Koobi Fora in northern Kenya confirm taxonomic diversity in early *Homo*. Nature. 488, 201-204.

Lordkipanidze, D., Ponce de León, M.S., Margvelashvili, A., Rak, Y., Rightmire, G.P., Vekua, A., Zollikofer, C.P.E., 2013. A Complete Skull from Dmanisi, Georgia, and the Evolutionary Biology of Early *Homo*. Science. 342, 326-331.

Madison, W.P., 1991. Squared-change parsimony reconstructions of ancestral states for continuous-valued characters on a phylogenetic tree. Syst. Zool. 40, 304-314.

Martins, E.P., Hansen, T.F., 1997. Phylogenies and the comparative method: A general approach to incorporating phylogenetic information into the analysis of interspecific data. Am. Nat. 149, 646-667.

Maureille, B., 1994. La face chez *Homo erectus* et *Homo sapiens*: recherche sur la variabilité morphologique et métrique, Anthropologie. Ph.D. Dissertation, Université de Bordeaux 1, Bordeaux.

McBrearty, S., Brooks, A.S., 2000. The revolution that wasn't : a new interpretation of the origin of modern human behavior. J. Hum. Evol. 39, 453-563.

Mellars, P., 1996. The Neanderthal Legacy. Princeton University Press, Princeton.

Mercier, N., Valladas, H., Joron, J.L., Reyss, J.L., Leveque, F., Vandermeersch, B., 1991. Thermoluminescence dating of the Late Neanderthal remains from Saint-Césaire. Nature. 351, 737–739.

Meyer, M., Fu, Q., Aximu-Petri, A., Glocke, I., Nickel, B., Arsuaga, J.-L., Martinez, I., Gracia, A., de Castro, J.M.B., Carbonell, E., Paabo, S., 2014. A mitochondrial genome sequence of a hominin from Sima de los Huesos. Nature. 505, 403-406.

Molleson, T., Cox, M., 1993. The Spitalfields Project volume 2-the anthropology, CBA research report. Council for British Archaeology, York.

Mounier, A., 2009. Validité du taxon *Homo heidelbergensis* Schoetensack, 1908. Ph.D. Dissertation Université de la Méditerrannée, Marseille.

Mounier, A., 2011. Définition du taxon *Homo heidelbergensis* Schoetensack, 1908 : analyse phénétique du massif facial supérieur des fossiles du genre *Homo* du Pléistocène moyen Bull. Mém. Soc. Anthropol. Paris. 23, 115-151.

Mounier, A., 2012. Le massif facial supérieur d'*Homo heidelbergensis* Schoetensack, 1908 : l'apport de la morphométrie géométrique Bull. Mém. Soc. Anthropol. Paris. 24, 51-68.

Mounier, A., Caparros, M., In Press. The phylogenetic status of *Homo heidelbergensis* – a cladistic study of Middle Pleistocene hominins. Bull. Mém. Soc. Anthropol. Paris. DOI: 10.1007/s13219-015-0127-4.

Mounier, A., Condemi, S., Manzi, G., 2011. The stem species of our species: A place for the archaic human cranium from Ceprano, Italy. PLoS ONE. 6, e18821.

Mounier, A., Marchal, F., Condemi, S., 2009. Is *Homo heidelbergensis* a distinct species? New insight on the Mauer mandible. J. Hum. Evol. 56, 219-246.

Oakley, K.P., 1964. The problem of man's antiquity. An historical survey. Bull. Br. Mus. Nat. Hist. Geology. 9, 171-172.

Pagel, M., 1999. The Maximum likelihood approach to reconstructing ancestral character states of discrete characters on phylogenies. Syst. Biol. 48, 612-622.

Pagel, M., 2002. Modelling the evolution of continuously varying characters on phylogenetic trees. In: MacLeod, N., Forey, P. L. (Eds.), Morphology, Shape and Phylogeny. CRC Press, pp. 269-286.

Paradis, E., Claude, J., Strimmer, K., 2004. APE: analyses of phylogenetics and evolution in R language. Bioinformatics. 20, 289-290.

Polly, P.D., 2001. Paleontology and the comparative method: ancestral node reconstructions versus observed node values. Am. Nat. 157, 596-609.

Polly, P.D., 2008. Adaptive zones and the pinniped ankle: a three-dimensional quantitative analysis of carnivoran tarsal evolution. In: Sargis, E., Dagosto, M. (Eds.), Mammalian Evolutionary Morphology. Springer Netherlands, pp. 167-196.

Polly, P.D., MacLeod, N., 2008. Locomotion in fossil carnivora: an application of eigensurface analysis for morphometric comparison of 3D Surfaces. Palaeontologica Electronica. 11, 10A:13p.

Pope, G., 1992. Craniofacial evidence for the origin of modern humans in China. Yearb. Phys. Anthropol. 35, 243-298.

Prat, S., 2004. Les premiers représentants du genre *Homo*, en quête d'une identité. Apports de l'étude morphologique et de l'analyse cladistique. Bull. Mém. Soc. Anthropol. Paris. 16, 17-35.

Prossinger, H., Seidler, H., Wicke, L., Weaver, D., Recheis, W., Stringer, C.B., Müller, G.B., 2003. Electronic removal of encrustations inside the Steinheim cranium reveals paranasal sinus features and deformations, and provides a revised endocranial volume estimate. Anat. Rec. 273 B, 132-142.

Prüfer, K., Racimo, F., Patterson, N., Jay, F., Sankararaman, S., Sawyer, S., Heinze, A., Renaud, G., Sudmant, P.H., de Filippo, C., Li, H., Mallick, S., Dannemann, M., Fu, Q., Kircher, M., Kuhlwilm, M., Lachmann, M., Meyer, M., Ongyerth, M., Siebauer, M., Theunert, C., Tandon, A., Moorjani, P., Pickrell, J., Mullikin, J.C., Vohr, S.H., Green, R.E., Hellmann, I., Johnson, P.L.F., Blanche, H., Cann, H., Kitzman, J.O., Shendure, J., Eichler, E.E., Lein, E.S., Bakken, T.E., Golovanova, L.V., Doronichev, V.B., Shunkov, M.V., Derevianko, A.P., Viola, B., Slatkin, M., Reich, D., Kelso, J., Paabo, S., 2014. The complete genome sequence of a Neanderthal from the Altai Mountains. Nature. 505, 43-49.

Reich, D., Green, R.E., Kircher, M., Krause, J., Patterson, N., Durand, E.Y., Viola, B., Briggs, A.W., Stenzel, U., Johnson, P.L.F., Maricic, T., Good, J.M., Marques-Bonet, T., Alkan, C., Fu, Q., Mallick, S., Li, H., Meyer, M., Eichler, E.E., Stoneking, M., Richards, M., Talamo, S., Shunkov, M.V., Derevianko, A.P., Hublin, J.-J., Kelso, J., Slatkin, M., Pääbo, S., 2010. Genetic history of an archaic hominin group from Denisova Cave in Siberia. Nature. 468, 1053-1060.

Revell, L.J., 2012. phytools: an R package for phylogenetic comparative biology (and other things). Met. Ecol. Evol. 3, 217-223.

Reyes-Centeno, H., Ghirotto, S., Détroit, F., Grimaud-Hervé, D., Barbujani, G., Harvati, K., 2014. Genomic and cranial phenotype data support multiple modern human dispersals from Africa and a southern route into Asia. Proc. Natl. Acad. Sci. 111, 7248-7253.

Rightmire, G.P., 1990. The Evolution of *Homo erectus*. Comparative Anatomical Studies of an Extinct Human Species. Cambridge University Press, Cambridge.

Rightmire, G.P., 1996. The human cranium from Bodo, Ethiopia: Evidence for speciation in the Middle Pleistocene? J. Hum. Evol. 31, 21-39.

Rightmire, G.P., 1998. Human evolution in the Middle Pleistocene : The role of *Homo heidelbergensis*. Evol. Anthropol. 6, 218-227.

Rightmire, G.P., 2008. *Homo* in the middle Pleistocene: Hypodigms, variation, and species recognition. Evol. Anthropol. 17, 8-21.

Rohlf, F.J., 2001. Comparative methods for the analysis of continuous variables: geometric interpretations. Evolution. 55, 2143-2160.

Rohlf, F.J., Slice, D.E., 1990. Extensions of the procrustes method for the optimal superimposition of landmarks. Syst. Zool. 39, 40-59.

Rosas, A., Bermúdez de Castro, J.M., 1998. The Mauer mandible and the evolutionary significance of *Homo heidelbergensis*. Geobios. 31, 687-697.

Schlager, S., 2013. Soft-Tissue reconstruction of the human nose: population differences and sexual dimorphism, Anthropologie. Ph.D. Dissertation, Universität Freiburg.

Schluter, D., Price, T., Mooers, A.Ø., Ludwig, D., 1997. Likelihood of ancestor States in adaptive radiation. Evolution. 51, 1699-1711.

Schoetensack, O., 1908. Der Unterkiefer des *Homo heidelbergensis* aus den Sanden von Mauer bei Heidelberg. Wilhelm Engelmann, Leipzig.

Seguin-Orlando, A., Korneliussen, T.S., Sikora, M., Malaspinas, A.-S., Manica, A., Moltke, I., Albrechtsen, A., Ko, A., Margaryan, A., Moiseyev, V., Goebel, T., Westaway, M., Lambert, D., Khartanovich, V., Wall, J.D., Nigst, P.R., Foley, R.A., Lahr, M.M., Nielsen, R., Orlando, L., Willerslev, E., 2014. Genomic structure in Europeans dating back at least 36,200 years. Science. 346, 1113-1118.

Smith, F.H., Jankovic, I., Karavanić, I., 2005. The assimilation model, modern human origins in Europe, and the extinction of Neandertals. Quatern. Int. 137, 7-19.

Spoor, F., Stringer, C.B., Zonneveld, F., 1998. Rare temporal bone pathology of the Singa calvaria from Sudan. Am. J. Phys. Anthropol. 107, 41-50.

Stringer, C., 2012. The status of *Homo heidelbergensis* (Schoetensack 1908). Evol. Anthropol. 21, 101-107.

Stringer, C.B., 1983. Some further notes on the morphology and dating of the Petralona hominid. J. Hum. Evol. 12, 731-742.

Tamrat, E., Tohveny, N., Taieb, M., Opdyke, N., 1995. Revised magnetostratigraphy of the Plio-Pleistocene sedimentary sequence of the Olduvai Formation (Tanzania). Palaeogeogr. Palaeoclimatol. Palaeoecol. 114, 273-283.

Tattersall, I., Schwartz, J.H., 2006. The distinctiveness and systematic context of *Homo neanderthalensis*. In: Harvati, K., Harrison, T. (Eds.), Neanderthals Revisited. Springer, New York, pp. 9-22.

Teixeira, A.S., Monteiro, P.T., Carriço, J.A., Ramirez, M., Francisco, A.P., 2015. Not seeing the forest for the trees: size of the minimum spanning trees (MSTs) forest and branch significance in MST-based phylogenetic analysis. PLoS ONE 10, e0119315.

Toussaint, M., Pirson, S., 2006. Neandertal studies in Belgium: 2000-2005. Period. Biol. 108, 373-387.

Trinkaus, E., 1983. The Shanidar Neanderthals. Academic Press, New York.

Trinkaus, E., 1991. Les hommes fossiles de la Grotte de Shanidar, Irak: évolution et continuité parmi les hommes archaïques tardifs du Proche-Orient. L'Anthropologie. 95, 535–572.

Vandermeersch, B., 1981. Les Hommes de Qafzeh (Israël). CNRS, Paris.

Villmoare, B., Kimbel, W.H., Seyoum, C., Campisano, C.J., DiMaggio, E., Rowan, J., Braun, D.R., Arrowsmith, J.R., Reed, K.E., 2015. Early *Homo* at 2.8 Ma from Ledi-Geraru, Afar, Ethiopia. Science. 347, 1352-1355.

Wagner, G.A., Krbetschek, M., Degering, D., Bahain, J.-J., Shao, Q., Falguères, C., Voinchet, P., Dolo, J.-M., Garcia, T., Rightmire, G.P., 2010. Radiometric dating of the type-site for *Homo heidelbergensis* at Mauer, Germany. Proc. Natl. Acad. Sci. 107, 19726-19730.

Weaver, T.D., Roseman, C.C., Stringer, C.B., 2007. Were Neandertal and modern human cranial differences produced by natural selection or genetic drift? J. Hum. Evol. 53, 135-145.

Weaver, T.D., Roseman, C.C., Stringer, C.B., 2008. Close correspondence between quantitative- and molecular-genetic divergence times for Neandertals and modern humans. Proc. Natl. Acad. Sci. 105, 4645-4649.

Wiley, D.F., 2005. Landmark v 3.0. Institute for Data Analysis and Visualization. University of California, Davis.

Wiley, D.F., Amenta, N., Alcantara, D.A., Ghosh, D., Kil, Y.J., Delson, E., Harcourt-Smith, W., Rohlf, F.J., St. John, K., Hamann, B., 2005. Evolutionary Morphing, Proceeding of IEEE Visualization 2005.

Wolpoff, M.H., Thorne, A.G., Smith, F.H., Frayer, D.W., Pope, G.G., 1994. Multiregional evolution: a world-wide source for modern human populations. In: Nitecki, M.H., Nitecki, D.V. (Eds.), Origins of Anatomically Modern Humans. Plenum Press, New York, pp. 175-199.

Wood, B., 1999. '*Homo rudolfensis*' Alexeev, 1986-fact or phantom? J. Hum. Evol. 36, 115-118.

Wood, B., Lonergan, N., 2008. The homini fossil record: taxa, grades and clades. Journal of Anatomy. 212, 354-376.

Wood, B.A., 1993. Early *Homo*. How many species ?. In: Kimbel, W.H., Martin, L.B. (Eds.), Species, Species Concepts, and Primate Evolution. Plenum Press, New York and London, pp. 485-522.

Supplementary Data:

Appendix A: Virtual Last Common Ancestor estimation

Table legends

Table A.1. PC statistics of the Principal Component Analysis used to compute the ancestral states.

Appendix B: 3D pdfs of vLCA1, vLCA2, vLCA3

Virtual LCAs to *H. sapiens* and *H. neanderthalensis* for the three distinct chronological models: late Lower Pleistocene common ancestry (model 1), early Middle Pleistocene common ancestry (model 2), and mid-Middle Pleistocene common ancestry (model3). The 3D pdfs were created using Geomagic Studio (v12.0.0 © 2010 Geomagic, Incorporated and its licensors).

Appendix C: Geometric morphometric analysis of the vLCAs

Table legends

Table C.1. Landmarks used in the geometric morphometric analyses of the calvarium.

Number, name, description and type for each landmark of the calvarium.

Table C.2. Landmarks used in the geometric morphometric analysis of the upper face.

Number, name, description and type for each landmark of the upper face.

Table C.3. Main PCs statistics from the PCA of the calvarium and of the upper face

Eigenvalues, percentage of variance and cumulative variance for each principal component of the tow analyses.

Appendix D: 3D pdfs of full bilateral models of vLCA1, vLCA2 and vLCA3

Full bilateral reconstruction of the virtual LCAs to *H. sapiens* and *H. neanderthalensis* for the three distinct chronological models: late Lower Pleistocene common ancestry (model 1), early Middle Pleistocene common ancestry (model 2), and mid-Middle Pleistocene common ancestry (model3). The bilateral reconstruction are based on the original sets of landmarks which have been mirrored and retro-deformed (R Morpho package version 2.1, Schlager, 2013). The 3D pdfs were created using Geomagic Studio (v12.0.0 © 2010 Geomagic, Incorporated and its licensors).